1STRESS INTENSITY FACTORS FOR EMBEDDED CRACKS WITHIN TORSIONALLY LOADED SQUARE PRISMATIC BARS

ZHOU DING

FACULTY OF ENGINEERING
UNIVERSITY OF MALAYA
KUALA LUMPUR

2016

STRESS INTENSITY FACTORS FOR EMBEDDED CRACKS WITHIN TORSIONALLY LOADED SQUARE PRISMATIC BARS

ZHOU DING

DISSERTATION SUBMITTED IN FULFILMENT OF THE
REQUIREMENTS FOR THE DEGREE OF
MASTER OF ENGINEERING SCIENCE

FACULTY OF ENGINEERING
UNIVERSITY OF MALAYA
KUALA LUMPUR

2016

UNIVERSITY OF MALAYA
ORIGINAL LITERARY WORK DECLARATION

Name of Candidate: **ZHOU DING**

Registration/Matric No: **KGA140050**

Name of Degree: **MASTER OF ENGINEERING SCIENCE**

Title of Project Paper/Research Report/Dissertation/Thesis ("this Work"):

STRESS INTENSITY FACTORS FOR EMBEDDED CRACKS WITHIN TORSIONALLY LOADED SQUARE PRISMATIC BARS

Field of Study: **ENGINEERING DESIGN-FRACTURE MECHANICS**

I do solemnly and sincerely declare that:

(1) I am the sole author/writer of this Work;
(2) This Work is original;
(3) Any use of any work in which copyright exists was done by way of fair dealing and for permitted purposes and any excerpt or extract from, or reference to or reproduction of any copyright work has been disclosed expressly and sufficiently and the title of the Work and its authorship have been acknowledged in this Work;
(4) I do not have any actual knowledge nor ought I reasonably to know that the making of this work constitutes an infringement of any copyright work;
(5) I hereby assign all and every rights in the copyright to this Work to the University of Malaya ("UM"), who henceforth shall be owner of the copyright in this Work and that any reproduction or use in any form or by any means whatsoever is prohibited without the written consent of UM having been first had and obtained;
(6) I am fully aware that if in the course of making this Work I have infringed any copyright whether intentionally or otherwise, I may be subject to legal action or any other action as may be determined by UM.

Candidate's Signature Date:

Subscribed and solemnly declared before,

Witness's Signature Date:

Name:

Designation:

ABSTRACT

Solid bars are widely used in engineering applications for machine components and structures. Since the presence of an embedded crack in a solid bar could lead to a catastrophic failure of a whole structure, relevant studies on evaluating quantitative fracture values are always sought for the improvement of design in components. Due to the complexity of the experimental setup for evaluating an embedded crack in a solid component, numerical modelling becomes an attractive solution. Up to this date, only few studies of evaluating the stress intensity factors for the embedded cracks in a solid bar are reported in literature. Therefore, this research focuses on the evaluation of the stress intensity factors (SIFs) of an elliptical embedded crack in a square prismatic metallic bar subjected to torsion loading. To this end, the effects of various crack parameters on SIFs are investigated: crack aspect ratio, crack inclination and crack eccentricity. A software package of the boundary element method (DBEM) named BEASY is utilized to perform the analyses. *J*-integral method is adopted in order to compute the SIFs. Results show that as the crack aspect ratio increases, the absolute value of K_2 increases while K_3 decreases. Moreover, by evaluating 8 eccentricity values, it is found that K_2 and K_3 increases with the crack eccentricity. Through numerical analysis, it is revealed that for the case of inclined crack, the inclination angle of 45 degree produces maximum value of K_1. Finally, the numerical findings are related to the stress distribution in the cross section of square bar using the theory of elasticity.

ABSTRAK

Bar pepejal luas digunakan dalam aplikasi kejuruteraan untuk komponen mesin dan struktur. Memandangkan kemunculan retakan yang terbenam di dalam bar pepejal boleh menyebabkan kegagalan struktur keseluruhan, penyelidikan yang relevan terhadap penilaian kuantitatif bagi nilai patah sentiasa diusahakan untuk mempertingkatkan rekaan bentuk komponen. Oleh sebab persediaan eksperimen untuk menilai retakan terbenam di dalam komponen pepejal yang terlalu rumit, pemodelan berangka menjadi satu penyelesaian yang menarik perhatian. Hanya beberapa penyelidikan dijalankan untuk menilai faktor keamatan tekanan atas retakan terbenam di dalam bar pepejal yang dilaporkan di dalam kesusasteraan sehingga kina. Oleh demikian, penyelidikan ini memberi tumpuan kepada penilaian faktor keamatan tekanan (SIFs) daripada retakan terbenam berbentuk elips di dalam bar logam prismatik persegi tertakluk terhadap kilasan muatan. Kesan-kesan pelbagai parameter keretakan SIFs telah dikaji untuk mencapai objektif ini, merangkumi nisbah aspek retakan, kecenderungan retakan dan kesipian retakan. Sebuah pakej perisian kaedah unsur sempadan (DBEM) yang dinamakan BEASY telah digunakan untuk mejalankan analisis dalam penyelidikan ini. Kaedah J-integral diamalkan untuk mencari nilai SIFs. Keputusan menunjukkan bahawa pernambahan nisbah aspek retakan akan meningkatkan nilai mutlak bagi K_2 tetapi menurunkan nilai K_3. Selain itu, didapati bahawa nilai K_2 dan K_3 meningkat dengan kesipian retakan berdasarkan penilaian terhadap 8 nilai kesipian. Melalui analisis berangka, ia dinyatakan bahawa sudut kecondongan 45 darjah akan menghasilkan nilai maksimum K_1 dalam kes retakan cenderung. Akhir kata, hasil kajian berangka ini berkaitan rapat dengan agihan tegasan dalam keratan rentas bar persegi dengan menggunakan teori keanjalan.

ACKNOWLEDGMENTS

I would like to express my immense indebtedness and gratitude to my supervisors Associate Prof. Dr. Andri Andriyana, Dr. Liew Haw Ling as well as Associate Prof. Dr. Judha Purbolaksono for their support, guidance, valuable comments, ideas and motivation that helped me in conducting my research and in completion of this dissertation.

I would express special gratitude to Mr. Muhammad Imran and Ms. Zhou Shanshan for the help and advices during the completion of this study. Sincere thanks to CAD/CAM lab technicians and my colleagues for their cooperation and support throughout this study.

I wish to thank Dr. Noor Azizi Bin Mardi and the Ministry of Higher Education, Malaysia, through the High Impact Research Grant (UM.C/625/1/HIR/MOHE/ENG/33) to provide funding for this research.

Finally, it would be understated to say thanks to my mother and my grandparents, as I consider it beyond myself to express such feelings for them in always being there as source of encouragement and inspiration.

Zhou Ding

June, 2017

DECLARATION

I certify that this research is based on my own independent work, except where acknowledged in the text or by reference.

No part of this work has been submitted for any degree or diploma to this or any other university.

ZHOU DING

Supervisors: Associate Prof. Dr. Andri Andriyana

Department of Mechanical Engineering
Faculty of Engineering
University of Malaya
Kuala Lumpur
Malaysia

Dr. Liew Haw Ling

Department of Mechanical Engineering
Faculty of Engineering
University of Malaya
Kuala Lumpur
Malaysia

TABLE OF CONTENTS

LIST OF FIGURES

LIST OF TABLES

LIST OF SYMBOLS

a crack length of embedded crack

A half of the width of the rectangular bar

b crack depth of an embedded crack

B half of the height of the rectangular bar

C an elliptical contour

d diameter of the cylinder bar

e eccentricity (offset) of crack from centroid

E Young's modulus

G shear modulus

K_0 nominal stress intensity factor

K_1 Mode I stress intensity factor

K_2 Mode II stress intensity factor

K_3 Mode III stress intensity factor

L thickness of the component

m outward normal vector

M torque

N No. of cycles

S an arbitrary closed contour

W strain energy per unit volume

x a boundary point

x' a source point

X axis X

X' axis X'

α inclination of crack

θ angle of twist per unit length

υ Poisson ratio

σ applied shear stress

τ shear stress

$\hat{\tau}$ normalized shear stress

ΔK stress intensity factor range

φ scalar stress function

$\emptyset$ diameter of the cylinder bar

LIST OF ABBREVIATIONS

COD	Crack opening displacement
DBEM	dual boundary element method
FEA	finite element analysis
LEFM	Linear elastic fracture mechanics
NLEFM	Non-linear elastic fracture mechanics
PDD	parametric dislocation dynamics
SIF	stress intensity factor

CHAPTER 1

INTRODUCTION

1.1 Introduction

Square prismatic components are widely used in many industries such as construction, automotive, offshores, oil and gas, machineries, power plant, electrical power, and interior design. Prismatic components used as mold template, mortise pin, and column. The solid bars are widely used in engineering applications for machine components and structures. Manufacturing processes and loading during services could promote the initiation of an embedded crack in these components. The crack may then propagate when the components are operated under repeated, alternating or fluctuating stresses. Nowadays fracture mechanics analysis plays an important role in designing industrial components and has become important requirement for releasing the products. Hence, the study on fracture mechanics is important to understand the crack behaviors in materials in order to improve the mechanical performance of the products. As the prismatic bars are widely used in many industries such as structures in engineering applications and components in mechanical structure of machines, embedded cracks are often found in solid bars during services. These flaws cause the reduction of mechanical strength of the solid bars and could lead to a disastrous failure of the structure. Since fracture mechanics perspective has widely been adopted in engineering design process, studies on the stress intensity factor have become necessary, especially the possibility of the use of the data in a preliminary design stage. Relevant solutions/data are always sought to support the use of non-destructive technique for evaluating the embedded defects in structures. However, as reported by Lee (2007), there are only few studies on the embedded elliptical crack in solid bars that have been reported in literature. This statement was also highlighted by

Atroshchenko, Potapenko, and Glinka (2009) who noted that an embedded elliptical crack is more complex and challenging in crack geometry in comparison to surface cracks.

In real events, this low energy fracture in high strength materials invigorated the advanced improvement of fracture mechanics. Fracture mechanics is an important tool to assess the behavior of component containing pre-existing crack. The object of fracture mechanics is to give quantitative responses to specific issues concerning cracks in structures. The role of fracture mechanics is illustrated in Figure 1.1.

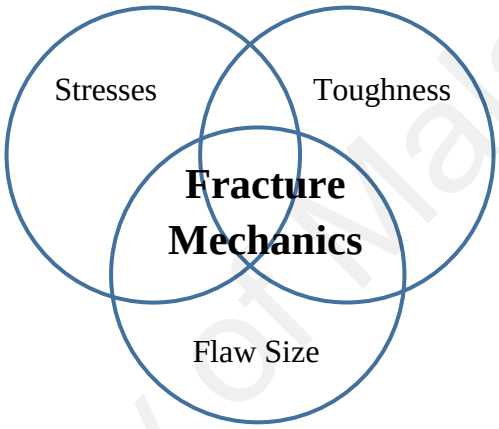

Figure 1.1: Facture Mechanics consist of effects from stress status, material nature and flaw property. (Speck, 2005)

As an outline, consider a structure containing prior imperfections and/or in which cracks start in industrial adaption. The cracks might develop with time attributable to different reasons (for instance fatigue, wear, stress erosion) and will for the most part become logically quicker as depicted in Figure 1.2(a). The residual strength of the structure, which is the failure strength as an element of split size, diminishes with expanding crack size, as appeared in Figure 1.2(b). After a period, the residual strength turns out to be low to the point that the structure might fall flat in service (Janssen, 2004).

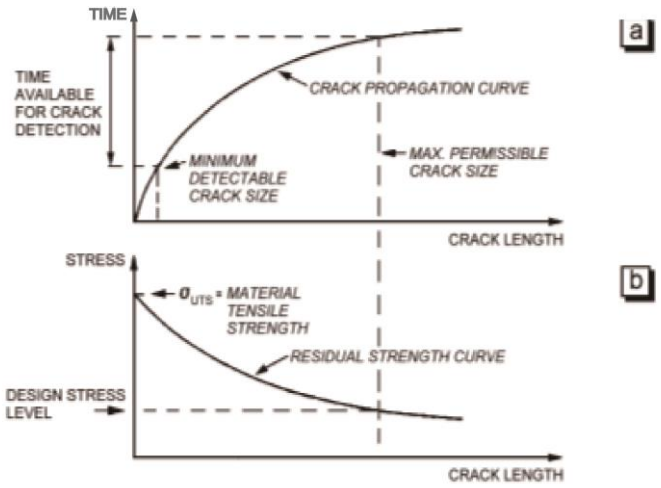

Figure 1.2: Engineering relationship with a crack. (Janssen, 2004)

Also as we can see from the Figure 1.3, fracture mechanics which is considered with even ideal prospect is always widespread used in applications in our life, such as in aviation, machinery, chemical industry, shipbuilding, transportation as well as military project fields. It is solving the fracture resistance design, material selection, formulating the suitable heat treating and manufacturing processes, predicting fatigue life of components, modeling acceptable quality checking criterion and maintenance steps as well as fracture preventing and so many other problems. From the microscopic aspect, fracture mechanics researches misplaced atoms and the fracture processes of microscopic structure which is even smaller than crystalline grain, and in terms of the understanding of these processes, establishes supporting criteria for crack propagation and fracture. In contrast, from the macroscopic aspect, it makes evaluation and controlling for fracture intensity via analyzing the continuous medium mechanics and experimenting components excluded the condition for the fracture mechanism inside of materials. Hence, it is a highly valuable subject in application.

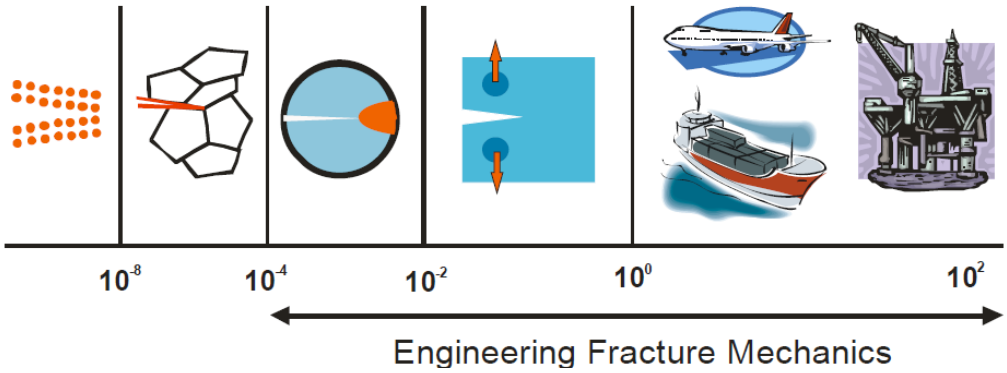

Figure 1.3: Fracture mechanics widespread use. (Janssen, 2004)

As embedded crack evaluation in fracture mechanics research poses formidable challenges for both analytical and experimental solutions. The state of the art for material cutting and joining is perhaps still too limiting for creating experimental samples with embedded crack; and samples deliberately obtained by controlling metallurgical processing are often too difficult to study as crack density, size, location, and orientation almost never appeared favorably for experimental purposes. On the other hand, the analytical formulation of the boundary value problem for embedded elliptical crack is complex and challenging; and it is only amenable for special geometry and loading conditions. So, the way to do the figure the research out by simulating analysis would be efficient and valid. Hereby, we presented the results for the SIFs of embedded elliptical cracks within square prismatic bars under torsion. The lack of available solutions of such has been reported in literature to date. The effects of elliptical aspect ratio, eccentricity in the sense of an offset from the cross-sectional centroid, and inclination with respect to the plane normal to the centroid axis are studied. By way of an effective sampling of crack's offset location and the regularity of the stress field, a reasonable ball-park estimate of SIFs for a crack at any location could be inferred using the results presented. All simulation results are performed using BEASY (2013), a relatively new program based on the dual boundary element method (DBEM).

1.2 Objectives

A. To investigate numerically the effects of different crack parameters including crack aspect ratio, crack eccentricity and crack inclination on the stress intensity factor (SIF) of embedded cracks in a square bar under torsion loading.
B. To evaluate the stress intensity factors (SIFs) for embedded cracks in square prismatic bars under torsion loading and analysis the reasons and effects of them.

1.3 Scope of the research

Main focus of this work is to assess the stress intensity factor value of embedded cracks under cyclic torsion loading as well as to investigate the effects of crack parameters as following:

Crack aspect ratio, crack eccentricity, parametric crack size and crack inclination, as well as the different geometry of model comparisons. No experimental work was conducted.

1.4 Dissertation organization

This study report involves six parts which are showed as the following:

Chapter 1: *Introduction*: this section displays the brief foundation and significance of the exploration. The scope and objectives of this research is additionally characterized in this section.

Chapter 2: *Literature Review:* This section discusses about the fundamentals of Fracture mechanics, stress intensity factors and theory of finite or boundary element method and pervious works done by different analysts to assess SIFs, different strategies set up to deal with the crack mechanics issues is basically concluded and reported.

Chapter 3: *Methodology:* This section illustrates the method took after to accomplish the designed destinations, software of BEASY programming wizard and its applications.

Chapter 4: *Results and Discussion:* This part shows, firstly, the benchmarking of BEASY results with accessible results in the previous work followed by the use of the Theory of Elasticity that could explain the reason of the effect of SIFs performed on the square bar. Moreover, the effects of the crack aspect ratios, crack eccentricities and the crack inclinations are discussed. Lastly, the remark study also showed the effect of the geometry of different models.

Chapter 5: *Conclusions:* This part summarizes all the research finding and provides insight into suggested future work.

CHAPTER 2

LITERATURE REVIEW

2.1 Introduction

Prismatic bars are ubiquitously used as structural components in mechanisms, machineries, and other engineering applications. Embedded crack often found in prismatic bar during it application at different industries. Fatigue failure will occur in that particular embedded crack prismatic bar when the crack remains undiscovered and continue its application which load applied. Loading during services and manufacturing processes can also promote an embedded crack that typically often initiates in these components. It then may grow and cause the fatigue failure of the component under applied static loads. Selection of material and inspection routine playing an important role to avoid fatigue failure occur in components or structures used in all industries. As engineers explore limits to design products, material defects and flaws must be examined and fracture analysis becomes essential. The approach of examining cracks using fracture mechanics requires the stress intensity factors (SIFs); relevant solutions and off-the-shelf data for such are often sought to develop, validate, and support non-destructive techniques for evaluation of embedded defects in solids. However, very few and limited studies on embedded elliptical cracks have been reported in literature. Hence, stress intensity factors are concerned in order to perform decision making in effective material selection and ensure efficient inspection routine are carried out. Fatigue crack behavior often used to linear elastic facture mechanics to analyze. The way to analyze the fatigue crack behavior has widely been linear elastic fracture mechanics (LEFM) approach nowadays where elastic stress-strain field in the vicinity of crack tip are normally evaluated by calculating the stress intensity factors. When stress intensity factor (SIF) is exceed SIF limit of prismatic bar's material, the cracked prismatic bar will propagate with load applied.

Currently there are only few studies for fracture mechanics of embedded crack in different locations in prismatic bar under pure torsion loading. Numerical analysis is a splendid option to investigate the stress intensity factor in order to obtain efficient and effective result.

2.2 Fatigue and failure

Under the cyclical loading, the permanent localized damage in one or more spots of materials, components and constructional elements would become cracks after a certain number of circulation. This sort of phenomenon is the typical fatigue in material and the crack would not even propagate until the fracture failure occurs as it's characteristics showed in Figure 2.1. The dark part on the cross section showed the final phenomenon after slow crack growth, the bright part is the sudden fracture intersection. Fatigue failure is a process of the damage accumulation, hence the mechanics feature of it is different with statics mechanics. First difference is that the failure will happen even if the cyclic stress is much less than the limitation of the statics mechanics (Kim & Laird, 1978), but it will not happen immediately, it takes some time and even more; Secondly, before the fatigue failure happens, there will sometimes not be any obvious residual deformation even if the plastic material with the ductility and malleability (Korkmaz, 2010).

Figure 2.1: Fracture failure of a mechanical component.

Theoretically speaking, there are three processes of the metal fatigue failure. Firstly, stage of microscopic crack: under the cyclic loading, due to the maximum stress of the objective usually emerges on the surface or near the surface location, the persistent slip band, grain boundary and inclusion of this range would develop to severe stress concentration spot and form the microscopic crack. After that, cracks would propagate along the $45°$ with the principal stress which is the maximal shear stress direction, the length of it would not exceed 0.05 mm, and the macroscopic crack is now developed. Secondly, stage of macroscopic crack derived by Paris, Gomez, and Anderson (1961): the crack generally would continue propagating along the perpendicular direction of the principal stress (Shigley et al., 1989). Lastly, stage of the sudden fracture: the objective would fracture immediately that subjected once more loading at any time when the crack propagates to a certain size of remaining cross section which would not resist the loading. These three stages could be plotted in Figure 2.2 below, where the failure due to fatigue in the form of the crack growth rate (da / dN) correlated with the cyclical component ΔK of the stress intensity factor K.

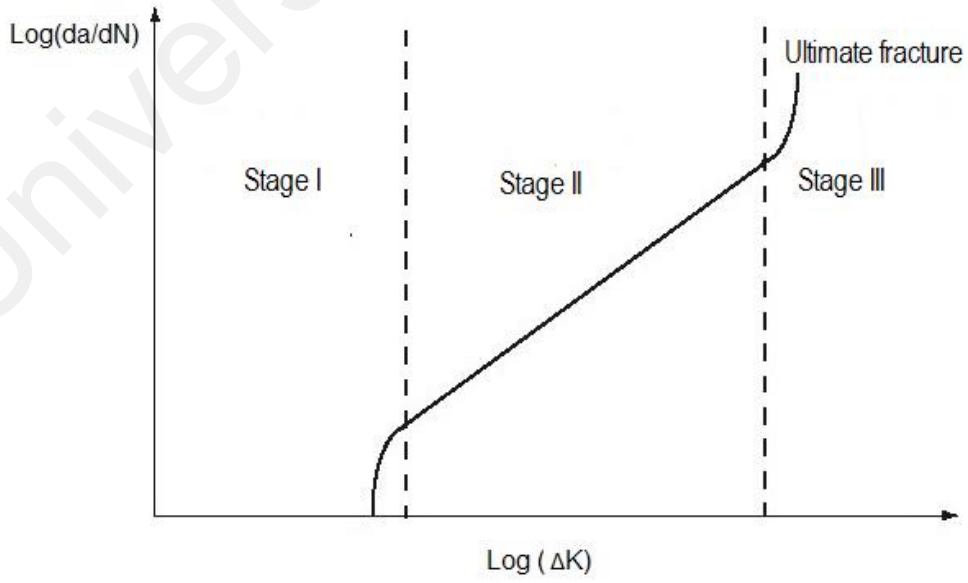

Figure 2.2: Stages of fatigue failure (Shigley et al.,1989)

There are many famous engineering accidents as Figure 2.3 showed that are investigated by researchers in theory of fatigue after graph of the magnitude of a cyclic stress against the logarithmic scale of cycles to failure (S-N curve) (Wöhler, 1870) is proposed (Rotem, 1991), so that the probable causes of these catastrophic disasters are valid to be found and it is also better for similar problems in other cases to refer to prevent earlier.

Few years ago, due to the crack growth of the structure, failures still happed. The shocked accident Sea Gem, as the first offshore oil rig in Britain before, resulted in 13 crews killed since the legs of its rig collapsed in 1965. Carson (1980) and Gramling and Freudenburg (2006) both pointed out that the collapse bought by the metal fatigue should never be used inside the suspension system to link the hull to rig legs and the fatigue failure is drowned with irreparable damage. The investigation of Hatfield rail crash on October of 2000 found by Vijayakumar, Wylie, Cullen, Wright, and Ai-Shamma'a (2009) also showed that rolling contact fatigue (also defined as multi-surface broke cracks) which is more severe than one single fatigue crack in a wheel in Eschede train disaster (Shallcross, 2013) caused a rail totally fragmented while trains were passing. Due the maintenance deficiency, there are so many gauge corner cracking with unknown location within the whole network that could lead to accident like above anytime. Fatigue cracks would not grow until the size of them reached a critical level, then the rail failed. Chetan, Khushbu, and Nauman (2012) reported that the fatal reason of the disaster of Chalk's Ocean Airways Flight 101 on December of 2005 was the fracture of the wing of the air plane resulted from the metal fatigue, and the problem is also due to the incorrect and inadequate way to detect and maintain the fatigue crack which is similar with the China Airlines Flight 611 accident in 2002 (W.-C. Li, Harris, & Yu, 2008). The fatigue failure brought the plane made in 1947 lost the right wing suddenly and rushed into the sea vertically during the flying process.

(a)

(b) (c)

Figure 2.3: (a) Sea Gem offshore oil rig; (b) Hatfield rail crash; (c) Chalk's Ocean Airways Flight 101

2.3 Fatigue design philosophies

To avoid the tragedies occurs, reliable design philosophy to prevent the fatigue-failure depends on experienced theories of mechanical engineering and material science. There are usually three criteria of design and evaluation utilized in fracture mechanics to assure the high quality of the design engineering product (Matthew, 2000):

2.3.1 Criterion of safe-life

This design promised the least probability of the fatigue failure without any inspection or maintenance for the component subjected varying load during the service life. This criterion is especially applied in aircraft field because of the difficulty of the repair and the severe disaster to the life that may cause, but the shortages of it would be the high cost and over designed.

2.3.2 Criterion of fail-safe

As the content in (Rutherford, 1992)said, the material is intended to withstand the most extreme static or cyclic working stresses for a specific period in a manner that its potential failure would not be calamitous. The target is to avert calamitous failure by recognizing and evaluating the crack at its initial phases of propagation.

2.3.3 Criterion of fault tolerance

After the supplement has been completed by Dubrova (2013), the main target of this criterion is assuming that the structure contained flaws from the manufacturing or service process, then analyze the changing process between the stress intensity factors and other parameters and fatigue loading within preexisting flaws assumed to ensure that the parameters would not exceed the critical value (fracture toughness) during the service life or overhaul period.

2.4 Fatigue and fracture mechanics

It would not be enough to predict the life of service or assure the reliability of the design based on empirical conclusion, life upgrading and design optimization are always desirable to be enhanced by using fracture mechanics (Freudenthal, 1973). According to Fischer-Cripps (2000), fracture mechanics is the theoretical principal for the theory of fault tolerance can be described briefly as “It aims to describe a material’s resistance to failure such as determination of material’s toughness”, and there are two specific

categories of it, one is linear elastic fracture mechanics, the other is elastic plastic fracture mechanics.

As a new branch of solid mechanics, fracture mechanics is one of the numerical analyses that researches the rules of cracks in materials and engineering structures especially for this kind of fatigue problem. Fracture mechanics studies the crack which is macroscopic and can be seen by eyes, and all kinds of flaws in engineering materials can be approximately regarded as crack. The content of fracture mechanics includes (Xing, 1991): Firstly, the initial condition of crack; Secondly, the propagation process of crack under external loading and/ or subjected to other factors; Last but not least, what kind of extent that crack would being propagating could lead the fracture of the objective. Furthermore, for the needy of engineering as criterion of fault tolerance demonstrated by Johnson (1984), what kind of condition could cause the fracture of the structure within crack; which size could be allowed to contain inside the structure under certain loading; the rest life of the structure under a certain circumstance within structure cracks or based on a kind of serving condition. Famous findings of fracture mechanics in history are shown in Figure 2.4.

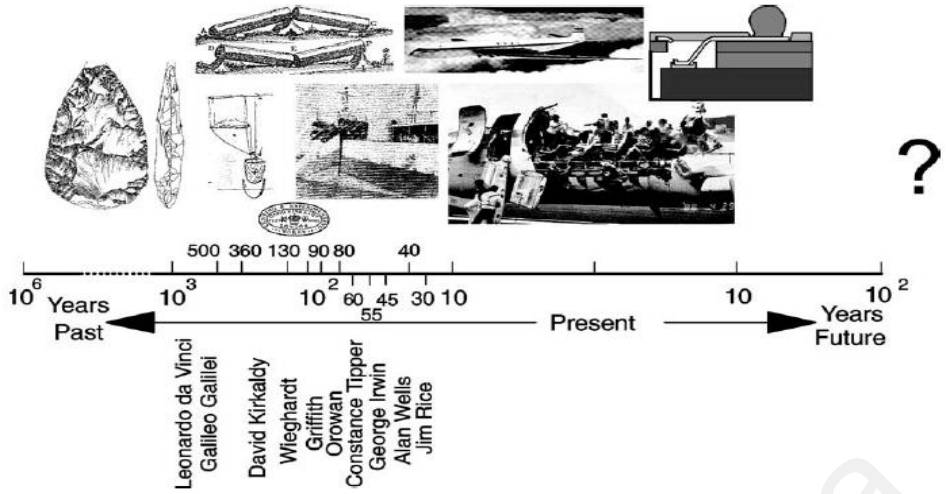

Figure 2.4: Brief history of fracture failure (Cotterell, 2002)

Many relevant studies have been done to contribute to the fracture mechanics research in fatigue field, also to find crack growth process and rules. As Figure 2.5 showed, generally, cracks are generated under the stress or environment effect within the material. No matter micro or macro-cracks are going to be propagated or enlarged under the external stress effect or/ and the external environment influence after the crack nucleation process, it is also called crack propagation or crack growth process. Cracks will result in the fracture of material after reached a critical extent.

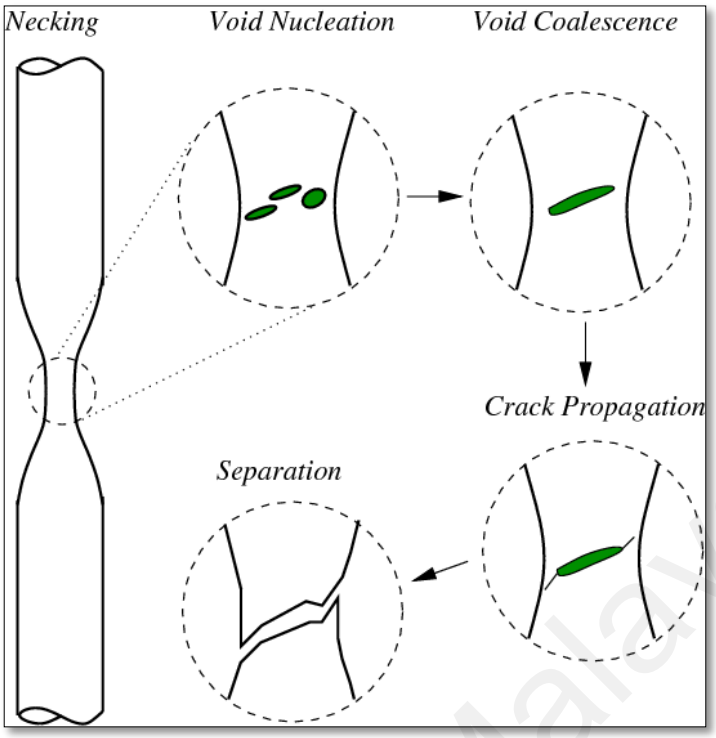

Figure 2.5: Fracture failure occurring steps

There is not only one type of crack within the material like the diagram showed above, but also other different types of it. Normally, corner crack, surface crack, and embedded crack as showing in Figure 2.6 are often found in material inspection.

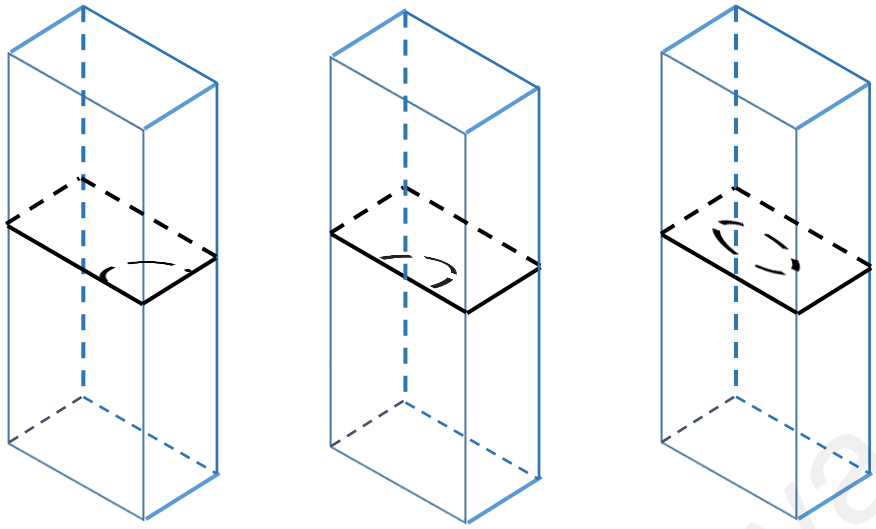

(a) (b) (c)

Figure 2.6: Crack within different locations of an objective (a) Corner crack (b) Surface crack (c) Embedded crack.

A crack in a component of a material is consist of disjoint one upper and one lower plane. The closed contour of the crack plane forms the crack front. When the objective within a crack is subjected to external loading, e.g. tension, bending or torsion. The crack faces would displace influenced by the loading with the deformed objective body, and in the meantime, the crack surfaces would be separated. This crack propagated phenomenon can be described as modes of failure. Three fracture modes that force the crack propagate resulted from applied loadings are illustrated in Figure 2.7: Mode I (K_1): Opening mode that the crack plane is perpendicular to tensile stress; mode II (K_2): in-plane shear that the crack plane is parallel to shear stress and the crack front is normal to the shear stress; mode III (K_3): out of plane tearing that the crack plane and the crack front are both parallel to the shear stress. Any fracture in a solid structure may be described due to subjecting any one or more of these three modes.

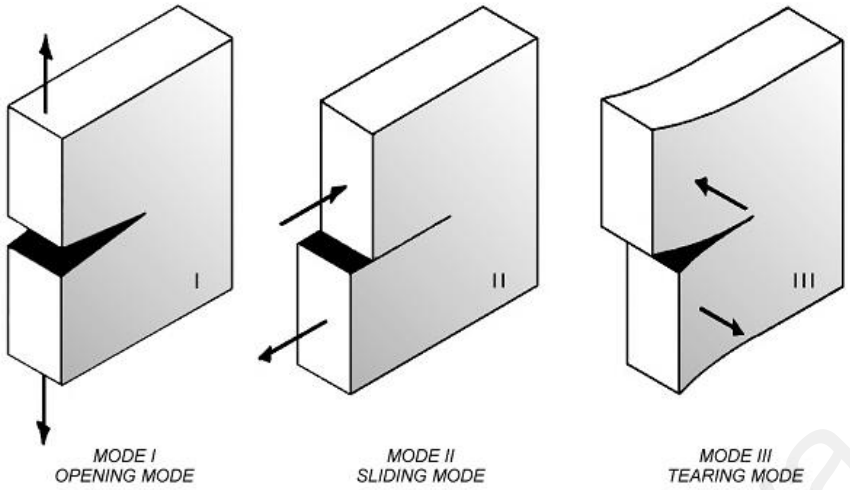

Figure 2.7: Crack separation modes

2.5 Linear Elastic Fracture Mechanics

As an important branch of the fracture mechanics, linear elastic fracture mechanics (LEFM) conducts the mechanics analyses for crack based on the linear theory of elastic mechanics, and adapts some characteristic parameters (e.g. stress intensity factor, energy releasing rate) obtained from analyses before as the criterion to evaluate the crack propagation. The study of LEFM is especially for brittle materials of which the internal plastic deformed is small during the crack propagation till the final fracture process.

The stress and strain acquired from LEFM are usually singular, which means the stress and strain on crack tip would be infinite. It is not logical in physics. In reality, the stress and strain near crack tip are high, LEFM is not applicable on crack tip. Generally speaking, these areas are complex, there are so many micro-factors (e.g. size of crystalline grain, dislocated structure, etc.) could affect the stress field of crack tip. The complex situation of crack tip would not be considered in LEFM, it applies the stress status of the outside area of crack tip to characterize the fracture features. When the external applied loading is not high, the fluctuate of the stress and strain near one of a small area of crack tip would

not influence the distribution of stress and strain of the external large area, and the stress and strain field affect in external small area could be settled by one parameter called stress intensity factor (SIF). For crack instability under this kind of loading effect, LEFM is applicable.

There two inequalities which ensure the LEFM applied loading value in terms of experiences(M. E. Erdogan, 2000)

$$a \geq 2.5\left(\frac{K_1}{\sigma_y}\right)^2 \tag{2.1}$$

$$L \geq 2.5\left(\frac{K_1}{\sigma_y}\right)^2 \tag{2.2}$$

Where a is the crack length; L is the thickness of the component; σ is the yield limit of material; K_1 is the safety intensity factor calculated by LEFM under external loading. In another word, K_1 has to satisfied with these two inequalities, as well, the effect of whole component should be linear under loading in LEFM.

There are couple of important theoretical achievements as following:

2.5.1 Griffith's criterion

During the World War I, fracture mechanics was still developed by Engineers. In terms of strain energy of crack in the objective, Griffith (1921) proposed the criterion of crack instability- Griffith's criterion. The criterion could explain the reason why the real fracture strength of glass is much less than the theoretical strength. Moreover, it became one of the basic conceptions of the linear elastic fracture mechanics later.

An object within a crack with length a as Figure 2.8 showed, the total potential energy of the object for every unit is $U(a)$ which is the function for crack length.

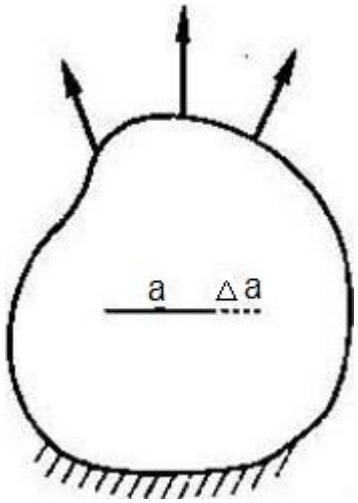

Figure 2.8: Object within crack

The total potential energy decreased when the crack length a is increasing, from which could be regarded as the crack propagation tendency result from external loading. The decreasing rate of potential energy with crack propagation is called crack propagation force or strain releasing rate, noted as *G*:

$$G = \lim_{\Delta a \to 0} \frac{U(a) - U(a+\Delta a)}{\Delta a} = -\frac{\partial U}{\partial a} \tag{2.3}$$

Under the external loading, the crack will not propagate even it showed propagation tendency until it reaches the certain value of the external loading; only the propagation occurs when the external loading increase to a critical value. Since in order to propagate the crack, the free surfaces should be increased, then the free surface energy also increased which amounted to the increment of resistance for the crack propagation. The crack will not propagate until the surface energy is adequate. Assuming the surface energy per unit is γ, crack length is *a*, then for the thickness per unit, the crack surface energy would be the function for crack length *a* below:

$$S = 2\alpha\gamma \tag{2.4}$$

The propagation resistance *R* could be measured by the changing rate between the surface energy and crack length, noted as:

$$R = \lim_{\Delta a \to 0} \frac{S(a+\Delta a) - S(a)}{\Delta a} = -\frac{\partial S}{\partial a} = 2\gamma \quad (2.5)$$

In summary, Griffith's criterion could be concluded as: crack propagation force equaling to crack propagation resistance (G=R) is the critical condition for crack propagating. This criterion successfully explained the brittle fracture problem of glass, but it is not suitably applicable for metal. However, it has been amended by Orowan (1949). He inputted the plastic work besides the surface energy. Then the criterion could also be applied on the metal to a certain extent after his amending.

2.5.2 Irwin's modification

During the World War II, fracture mechanics was developed even notably. Irwin (1997) presented the conception of stress intensity factor (SIF) via analyzing the stress field near crack tip area, and established crack propagation criterion based on SIF parameters, thereby successfully explained the brittle fracture accident with low stress. The toughness of plane strain is a significant parameter of the engineering safety design, the evaluation of it is the basic content of fracture mechanics since the status of plane strain is the most dangerous working status in real engineering structure.

As the polar coordinates showed in Figure 2.9, assuming both external loading and structure are symmetric with crack *a*. According to the calculation from elastic mechanics, the stress field near crack tip can be written approximately as following:

$$\sigma_x = \frac{K_1}{\sqrt{2\pi r}} \cos\frac{\theta}{2}\left(1 - \sin\frac{\theta}{2}\sin\frac{3\theta}{2}\right) \quad (2.6)$$

$$\sigma_y = \frac{K_1}{\sqrt{2\pi r}} \cos\frac{\theta}{2}\left(1 + \sin\frac{\theta}{2}\sin\frac{3\theta}{2}\right) \quad (2.7)$$

$$\tau_{xy} = \frac{K_1}{\sqrt{2\pi r}} \sin\frac{\theta}{2}\cos\frac{\theta}{2}\sin\frac{3\theta}{2} \quad (2.8)$$

Where σ_x, σ_y are stress components in a 2D problem; r and θ are polar coordinates. The approximate degree with equations above will be high if r is very small. Furthermore,

from the equations, we can conclude: stress will be increasing illimitably if $r \to 0$. K_1 is unrelated with r and θ, but the function for structure format and external loading, and it is also the parameter to control crack stress field. Irwin chose this one as a parameter to judge fracture which is called SIF.

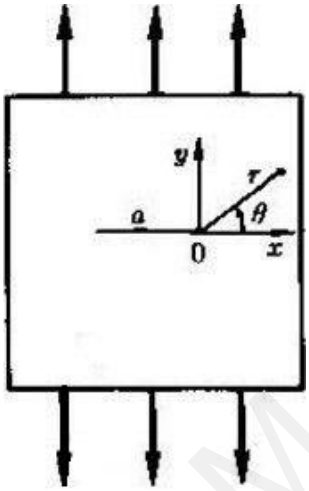

Figure 2.9: Polar coordinates of crack tip

2.6 Stress intensity factor

As a key point in LEFM, Irwin (1957) defined stress intensity factor (SIF) as a parameter to characterize the stress field strength near crack tip in elastic objective under external loading. According to LEFM above, any point near the crack in crack propagating process in Figure 2.10, the stress can be concluded as:

$$\sigma_{ij} = \frac{K}{\sqrt{2\pi r}} f_{ij}(\theta) \tag{2.9}$$

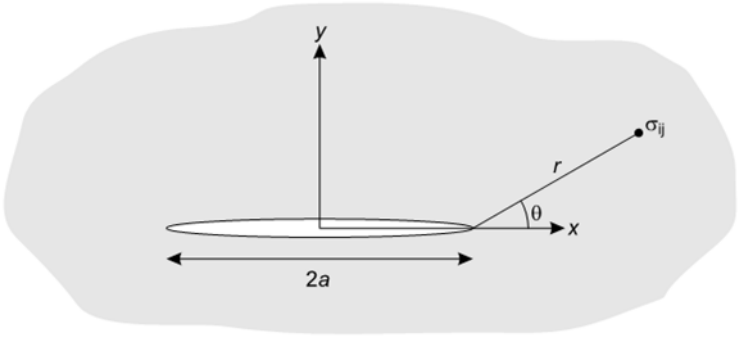

Figure 2.10: Stress at a point near crack tip

Where σij is the stress for a certain point; r and θ are the polar coordinates.

Recalling from the LEFM, the stress intensity factor in a finite crack objective is usually expressed as:

$$K = \sigma\sqrt{\pi a}\,.f(^{a}/_{W}) \tag{2.10}$$

Where *f (a/W)* is a function of boundary condition and a crack length about the geometry parameter.

And according to LEFM, the fracture failure would be recognized when SIF as high as a critical value K_c (also known as fracture toughness) which is written as

$$K_c = \sqrt{2E(\gamma_c + \gamma_p)} \tag{2.11}$$

Where E is Young's modulus, γ_c is the density of surface energy, and γ_p is the plastic strain energy.

Stress intensity factor plays a vital role to estimate the fatigue life of a structure or component. Therefore, there is an essential importance that robust and accurate method must be used to calculate stress intensity factor while predicting fatigue life of the component or structure with crack like defects.

2.7 Analytical solutions for crack problems

Most analytical methods to solve the SIF problems are complex functions or integral equations. Calculations for SIF values applied by variable functions in earlier time have been done by (Rooke, Cartwright, & Britain, 1976; Murakami, 1987) and many other researchers. Elliptical, semi-elliptical or quarter elliptical crack are used to define many cracks in engineering components and structures. The embedded crack in an infinite body subjected to external force is the most general case for elliptical flaw. Semi-circular/elliptical and quarter circular/elliptical cracks are also very common crack shapes in engineering fracture mechanics as they are commonly emanatedr from geometrical irregularities such as notches, sharp edges, pinhole, etc. Determination of SIFs for such cracks is actively sought in literature. The most well-known solutions were given by (Newman & Raju, 1983; Raju & Newman, 1986; Raju & Newman Jr, 1979). It is hard to find a simple analytical solution for other geometry and loading conditions in certain cases. Hence, numerical techniques are often needed in order to obtain precise model in the problems (Fischer-Cripps, 2000).

Montenegro, Cisilino, and Otegui (2006) utilized the O-integral algorithm and the weight function methodology for evaluating SIFs of embedded plane cracks. Wang and Glinka (2009) reported the stress intensity factors of embedded elliptical cracks under complex two-dimensional loading conditions using weight function method. Based on the properties of weight functions and the available weight functions for two-dimensional cracks, they proposed new mathematical expressions using the point load weight function.

Qian (2010) reported the effects of crack aspect ratio, crack eccentricity and effect of pipe thickness on the SIFs of an embedded elliptical crack axially oriented in a pressurized pipe using the interaction integral approach for three-dimensional finite element crack front model. In the same year, Livieri and Segala (2010) described an analytical methodology to calculate the Stress Intensity Factors (SIF) for planar embedded cracks

with an arbitrarily shaped front by using the celebrated integral of Oore–Burns with a first order expansion and the actual shapes of 3D planar flaws are analyzed based on the homotopic transformations of a reference disk.

Liu, Qian, Li, and Zheng (2011) calculated the stress intensity factors at the crack tip with the emphasis on the interaction between cracks for the double embedded elliptical cracks in a weld of pressure vessels under tension. It is found that the influence of the distance between the double embedded elliptical cracks and the differences with the single embedded crack of the point with maximum SIF. Takahashi and Ghoniem (2013) researched the SIF calculated by the Peach–Koehler (PK) force with numerical accuracy for penny-shape and elliptic cracks under pure Mode-I tension. Based on the Parametric Dislocation Dynamics (PDD) framework, the Burgers vector components corresponding to 3 modes in the PK force calculation could get the SIF simply done. In addition, the PDD method has also showed analogous fatigue crack growth to the dislocation dynamics simulations. Torshizian and Kargarnovin (2014) used plane elasticity theory to discuss an embedded arbitrarily oriented crack in a medium made of two dimensional functionally graded materials (2D-FGM) for the mixed-mode fracture mechanics analysis. What's more, they adapted the Fourier transformers to solve the partial differential equations into the Cauchy-type singular integral equations which was then solved using Gauss–Chebyshev polynomials. Finally, they solved Several different examples of SIFs with effects of nonhomogeneous material parameters $\delta 1$, $\delta 2$ and crack orientations θ and found the rules for the relationship between a combination of normal and shear loading applied on plate and a single normal loading for SIFs.

2.8 Numerical solutions for crack problems

As the computer technology nowadays is developing rapidly, it has enabled complicated and time consuming calculating became possible. Numerical solutions for the structure deformation and stress status are always more accurate than analytical solutions since it

contains more highly accurate details, such as element meshing, boundary condition and loading process etc. A lot of works to solve crack problems have been done by using numerical methods, and finite element method (FEM) and boundary element method (BEM) are two common ways.

2.8.1 Solutions by finite element method

It is often very important to estimate stress field around geometrical irregularities within any structure. Numerous studies on the usage of finite element method (FEM) to evaluate SIFs for structural discontinuities have been reported in literature. Yavari, Rajabi, Daneshvar, and Kadivar (2009) computed the resulting stress field in a rectangular plate with a pinhole and evaluated the effects of pin-plate clearance, friction, width of plate and position of hole using 2D FE model without incorporating the crack initiation and propagation mechanism. Lin and Smith (1999) researched finite element approach to evaluate two symmetric quarter elliptical cracks which located around the fastener holes subjected the pure tension and evaluated stress intensity factors by using J-integral method. The results were found to be in good agreements with previous literature. Da Fonte and De Freitas (1999) investigated a rotor shaft under mixed mode of torsion and bending loadings. The SIFs of the cracked shaft were accessed and the experimental data for validation were also compared. Next, Miranda, Meggiolaro, Castro, Martha, and Bittencourt (2003) used the FEM to evaluate the SIFs and fatigue growth analysis of one 2D structure using automatic re-meshing algorithm. Le Delliou and Barthelet (2007) presented the influence coefficients for plates containing an elliptical crack with the parameters: relative size, shape and free surface proximity for the distance from the center of the ellipse to the closest free surface by using Gibi to make the meshes and using the FEA program Code Aster to finish the calculation. RSE-M Code that provides rules and requirements for in-service inspection of French PWR components has accepted these solutions. R. Li, Gao, and Lei (2012) utilized the net-section collapse principle and the

commercial finite element software ABAQUS to illustrate the embedded off-set elliptical cracks in a plate under tension and bending combination loading. The new solutions are close to the elastic-perfectly plastic FEA results and conservative with less than 15% errors. Furthermore, the lower limit load has been studied by replacing a rectangular crack circumscribing the elliptical crack. Five cracked bars are introduced and estimated to analysis the cracked truss type of the structures, SIFs of simple cracks are calculated by following fracture mechanics laws in FEM (Yazdi & Shooshtari, 2014).

2.8.2 Solutions by boundary element method

However, finite element method above could be an expensive option in term of time of modelling as it requires treatments of meshing at the nearest location of the crack tip when evaluating stress field problems at the crack tip which involve singularities (Leonel, Venturini, & Chateauneuf, 2011). Hence, boundary element method (BEM) has become a suitable technique and an alternative tool in linear elastic fracture mechanics approach. It is simple in modelling desired crack and solutions obtained are accurate. Boundary element method able to solve stress concentration efficiently by mesh reduction features. Furthermore, it is more proficient in evaluating mixed mode crack growth models. Model boundaries are discretized in 2D problems, whereas, model surfaces are meshed in 3D problems. BEM stress equations identically satisfies throughout the structure volume different with FEM which used approximate equations. Quadratic boundary element is used in to evaluate various stress components (Trevelyan, 1992).

Many projects have applied BEM successfully by adapting the integral equation displacement boundary to structures without cracks. By using traction boundary integral equation, there are general solutions for different crack problems within geometry of three dimension (Domínguez & Ariza, 2000). Evaluation of stress intensity factor for various complex crack problems in elastic plate are presented by Yan (2006) by using displacement discontinuous element near crack tip based on boundary element method.

Next Yan (2010) implemented his previous work by using similar approach to evaluate multiple cracks problem in elastic media. Different methods applied by Wearing and Ahmadi-Brooghani (1999) to evaluate stress intensity factor. The methods that used such as displacement and stress extrapolation method, J-integral and quarter point approach are based on boundary element method. He proved that the results were in agreement with finite element solutions. Special emphasis on quarter point approach based on BEM was presented by Dong, Wang, and Wang (1997) to deal with interfacial crack model of two different materials. Yan and Liu (2012) evaluated stress intensity factors and elaborated the crack analysis of fatigue growth which was emanating from a circular hole in a plate of the elastic finite material. Atroshchenko et al. (2009) introduced the 3D classical elasticity for boundary value problem of an elliptical crack in an infinite body by using the method of simultaneous dual integral equations and solved the problem to transform to the linear algebraic equations system. They also obtained stress intensity factor (SIF) in the Fourier series expansion form. Hence, lots of specific cases under polynomial stress fields have got solutions and compared with previous results, then more complicated stress fields such as the partially loaded elliptical crack could also be figured out by adapting the method.

Choi and Cho (2014) developed an isogeometric shape design sensitivity analysis method for the stress intensity factors (SIFs) in curved crack problems. Based on this approach, they directly utilized the Non-Uniform Rational B-Splines (NURBS) basis functions in CAD system in the response analysis to enable a seamless incorporation of exact geometry and higher continuity into the computational framework. They presented several numerical examples of curved crack problems to verify the developed isogeometric analysis (IGA) method and design sensitivity analysis (DSA) of SIFs method through the comparison with solutions of the conventional finite element approach. Recently, Imran et al. (2015) solved the stress intensity factors for the

embedded (penny/elliptical) cracks that is also considered as the planar inclusion in a solid cylinder. They carried out all the analyses for the SIFs of an embedded crack for different crack aspect ratios, crack eccentricities and crack inclinations as well by using a dual boundary element method (DBEM) based software.

2.9 Boundary element method

The boundary element method (BEM) is a new numerical solution which is developing after the finite element method. It segments elements on the boundary of the domain of function which is quite different with the finite element method, of which the ideology is segmenting element in the continuum domain, and applies governing function to approximate the boundary condition. As pioneers, Jaswon, Maiti, and Symm (1967) have solved the potential problem based on the indirect boundary element method. Then, Rizzo (1967) figured out the 2D linear electrostatics problem used direct boundary element method. This kind of numerical solution then has been spread to 3D elasticity of mechanics by Cruse (1969). After that, Brebbia and Butterfield (1978) found the boundary integral equation through the derivation from weighted residual approach, he pointed out that the weighted residual approach must be the most general numerical method, and if regard Kelvin solution as the weighted function, then the boundary integral equation would be derived from weighted residual approach as the solution for the boundary element method, from which the theoretical system has been preliminarily formed. Boundary element method is now adapted in not only structure and mechanical field but also in sound field, electromagnetic field and so on as we can see from the Figure 2.11.

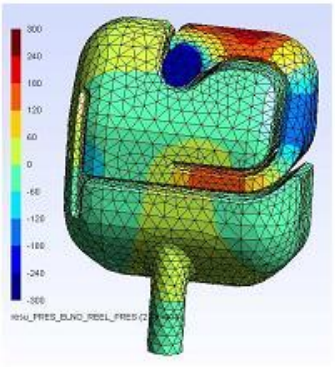

(a)

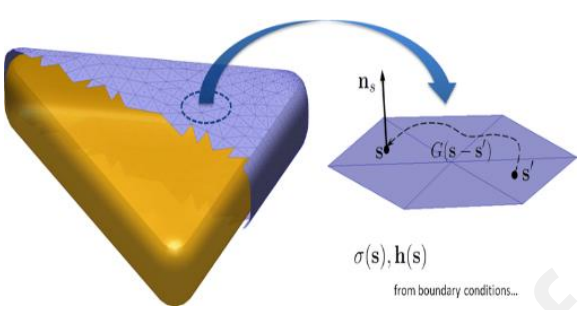

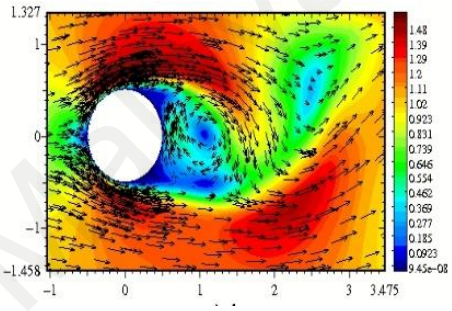

(b) (c)

Figure 2.11: Extensive use of BEM: (a) acoustics field (Brancati, Aliabadi, & Benedetti, 2009); (b) electromagnetic field (Hohenester & Trügler, 2012); (c) fluid mechanics field (Pasquetti & Peres, 2015)

2.9.1 Advantages of boundary element method

Boundary element method (BEM) has lots of benefits then other numerical methods that could be the premier option to solve the complex three dimensional problems in fracture mechanics area (Aliabadi, 1997; Costabel, 1987; Nageswaran, 1990). The advantages of it could be simply listed as following:

1. Less data preparation: BEM defined the boundary integral equation on the boundary as the governing function, it interpolates into the discrete function with the separable elements of the boundary and solve the boundary with the converted algebraic equations. Compared with the domain solution based on the partial

differential equation, the number of degrees of freedom is remarkably decreased because of the decreasing for the dimension of the problem, in the meantime, the solution of the discrete boundary could be considered much easier than the discrete domain. So the shape of the boundary can be simulated accurately with comparably sample elements and the final solution would be showed in the linear algebraic formulation with lower order.

2. Efficient modelling: The model creation here only for 2D wizard only asked the linked nodes. For 3D part, only patches connected every lines set previously are required which is totally different with else extruded volume programming packages. What's more, the amending for both 2D and 3D parts are easier because of the efficient modelling.

3. Easier meshing method: the model discretization for BEM is generally less time consuming. For the 2D cracks, the meshing method is only discretizing the surface with lines; the small regular surfaces are defined also easily to cover only the patches of the model for 3D objectives which could reduce the number of the dimension for the meshing problem.

4. More accurate results: Since the basis of the analysis for differential operator is used in BEM as the kernel function of the boundary integral equation, the feature of it supposed to concluded with combination of both analysis and value, then the accuracy of it is generally high, especially for the cases of boundary variable with high gradient changing, such as stress concentration problem, crack problem that the boundary variables appeared with singularities, and so on. BEM is universally acknowledged as more efficient with higher accuracy tool to solve the cased above than finite element method.

5. Special function for certain cases: boundary element method would be more convenient to handle the infinite domain and semi-infinite domain problems due to the differential operators used in BEM are satisfied in a condition of an infinite distance automatically.

2.9.2 Difficulties in boundary element method

1. Boundary integral equations require the explicit knowledge of a fundamental solution of the differential equation. Nonhomogeneous or nonlinear partial differential are not accessible by pure BEM.

2. Matrices of Boundary element formulation are not symmetric and fully dense. For computational analysis, it requires more storage and high computation speed.

2.10 Work flow of boundary element method

After 40 years researching and developing, BEM has already been an accurate and efficient analytical method of the numerical engineering. From the mathematical aspect, it has not only overcome the difficulty caused by the integral singularity in a certain extent, but also consolidated the convergence property, deviation analysis as well as other different kinds of mathematical BEM analyses so that the theoretical principal of BEM has been provided within the validity and reliability. When it comes to the application in diverse fields, there so many areas like engineering, science and technology have been spread. For linear problems, the application of BEM is already normalized; for nonlinear problems, the application of it is also going to be mature gradually. Figure 2.12 shows the steps of boundary element method.

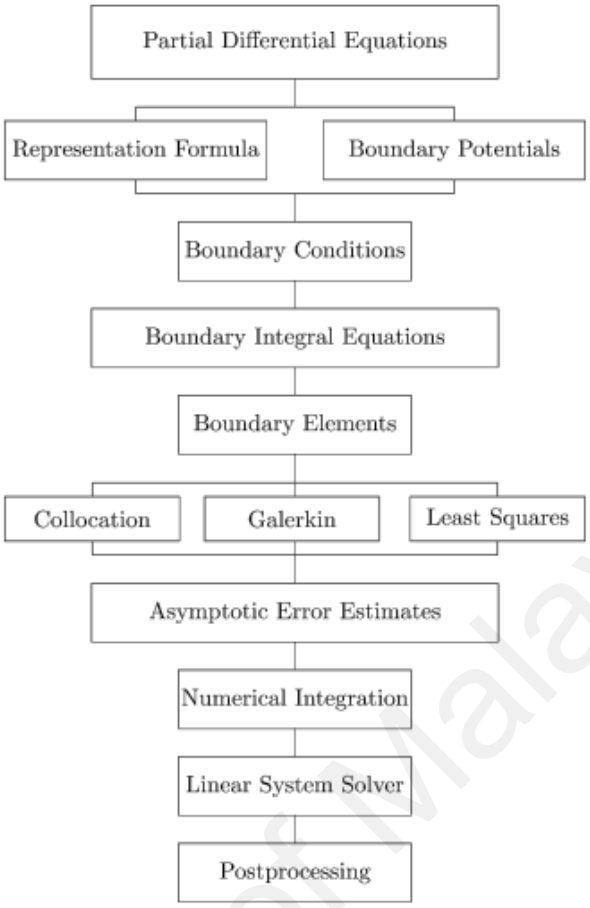

Figure 2.12: Flow chart of Boundary Element Method. (Hsiao, 2006)

2.11 Summary

Many methods are already available to calculate stress intensity factor values (F. Erdogan, 1983), especially for corner crack and surface crack. However, there are only few works on embedded crack that have been reported in literature (Lee, 2007).

Although the stress around geometrical irregularities has received extensive interests, the determination of stress field for different inclination degrees in several locations of embedded cracks remains open for updates. What's more, there is also only few analyses on solution for non-circular component such as square prismatic bar which pure torsion loading applied.

Many researchers have reported solutions for SIFs and fatigue growth analysis of simple geometry structures. However, no solutions in pure torsion loading of different aspect ratio of embedded crack in a square prismatic bar have been reported. This research is intended to specifically update the knowledge in fracture mechanics by evaluating the stress intensity factors of an embedded elliptical crack with different inclinations and to assess the stress intensity factors in several locations with different eccentricities, in order to update the knowledge in fracture mechanics by new designed model case. K_1, K_2 and K_3 rules under static conditions are implemented in following chapters.

CHAPTER 3

METHODOLOGY

3.1 Introduction

This section showed the techniques used to figure out the proposed objectives of this work. Stress intensity factor can be determined in three ways: experimentally, analytically and numerically. Experiment setups are hard to build up and significantly more tedious and immoderate. Analytical technique can ascertain exact SIFs just up to 2D crack issues. Because of the complexities in 3D crack geometries, experimental and analytical techniques are not as a suitable choice as that with the headway in computational simulation based programming software which is favored because of its comparably accurate and efficiency. As well, finite element method and boundary element method are most regularly utilized strategies compared to other numerical analysis method.

Furthermore, Boundary element method (BEM) is widespread used nowadays due to its multi benefits relative to finite element method. It is a developing technology to solve issues occurred in different parts of designing processes such as acoustics, fluid mechanics, thermal dynamics and electromagnetics as well as fracture mechanics and so on (Aliabadi, 1997). BEM and FEM have also been compared in some literatures previously (Citarella & Cricrì, 2010) and (Wanderlingh, 1986). Then the commercial software BEASY is actually one of the most popular tool based on boundary element method. BEASY programming is innovated to analyze fatigue, crack growth and flaw evaluation etc. In this work, BEASY programming is utilized to model, analysis and investigate for an embedded crack subjected to certain loading, such as, tension, torsion or the combination of these two.

3.2 Dual boundary element method in BEASY

Among these, from the application of the software, BEM applied software is going to develop to BEM programming package with preprocessor and postprocessor solving function and multi-problem dealing with. Dual boundary element method (DBEM) is now one of the most popular fatigue problem solving method and also used in the programming of BEASY software developed by Mi and Aliabadi (1992) which is used for computational engineering fracture analysis.

Stress intensity factors (SIFs) are evaluated in BEASY via the J-integral concept of (Rice, 1968) and (Cherepanov, 1967) which gives, for crack opening in the x_i direction, a path-independent energy integral of the form

$$J = \int_{\Gamma} \left(W n_i - t_k u_{k,i}\right) \mathrm{d}\Gamma \tag{3.1}$$

over a surface Γ with outward normal **n**. This concept was developed for linear elastic materials, and it was further extended to HRR solutions (Hutchinson, 1968) for materials with constitutive relationship in the form of Ramberg-Osgood. Using Green's functions U_{ij} for displacement and T_{ij} for traction, the strain energy density $W(\Gamma)$ and the work-conjugate of traction **t** and displacement **u** in J-integral are calculated using DBEM as follows (Mi and Aliabadi 1992).

$$u_i(\mathbf{x}') + \alpha_{ij}(\mathbf{x}')u_j(\mathbf{x}') + \int_{\Gamma} T_{ij}(\mathbf{x}', \mathbf{x})u_j(\mathbf{x})\mathrm{d}\Gamma(\mathbf{x}) = \int_{\Gamma} U_{ij}(\mathbf{x}', \mathbf{x})t_j(\mathbf{x})\mathrm{d}\Gamma(\mathbf{x}) \tag{3.2}$$

$$\frac{1}{2}t_j(\mathbf{x}') + n_i(\mathbf{x}') \int_{\Gamma} T_{ij,k}(\mathbf{x}', \mathbf{x})u_k(\mathbf{x})\mathrm{d}\Gamma(\mathbf{x}) = n_i(\mathbf{x}') \int_{\Gamma} U_{ij,k}(\mathbf{x}', \mathbf{x})t_k(\mathbf{x})\mathrm{d}\Gamma(\mathbf{x}) \tag{3.3}$$

where T_{ij}'s singularity of $O\left(\frac{1}{\|\mathbf{x}-\mathbf{x}'\|^2}\right)$ as $\mathbf{x} \rightarrow \mathbf{x}'$ warrants regularization and treatment in the sense of Cauchy; and $\alpha_{ij}(\mathbf{x}')$is a term that emanates heretofore from an integral with the fundamental solution T_{ij} as its kernel. They claimed to have presented an effective numerical implementation of the dual boundary integrals, and such is BEASY.

3.3 Simulation Work

3.3.1 Model geometry and property

As Figure 3.1 showed below, this simulation for the SIFs uses a prismatic square bar with the cross-section of $10 \times 10\ \text{mm}^2$ and length of 40 mm. It is twisted with a torque M_t that corresponds to the maximum shear stress of $\tau_{\max} = 100$ MPa. An isotropic linear elastic material mild with Young's modulus of 210 GPa and Poisson's ratio of 0.29 is used, such stiffness moduli are typical for steel alloys.

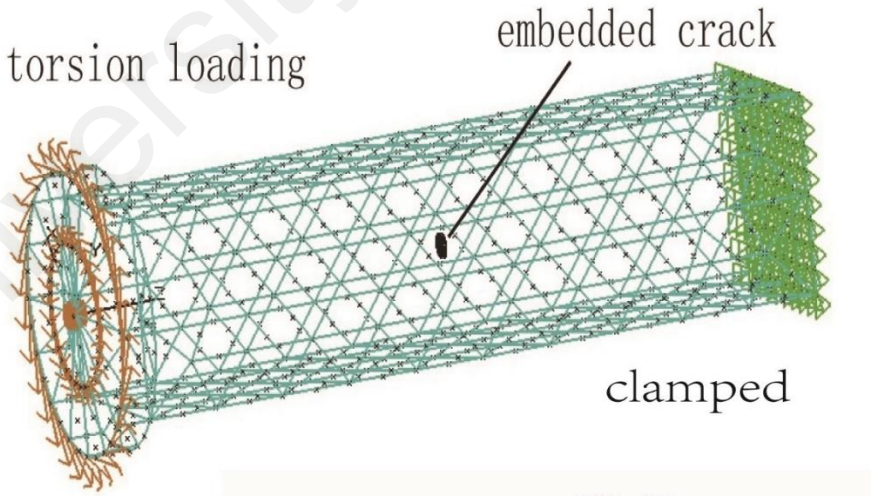

Figure 3.1: The square prismatic bar within an embedded crack used in this work

3.3.2 BEASY working processes

The working processes of the software BEASY is illustrated as following in Figure 3.2.

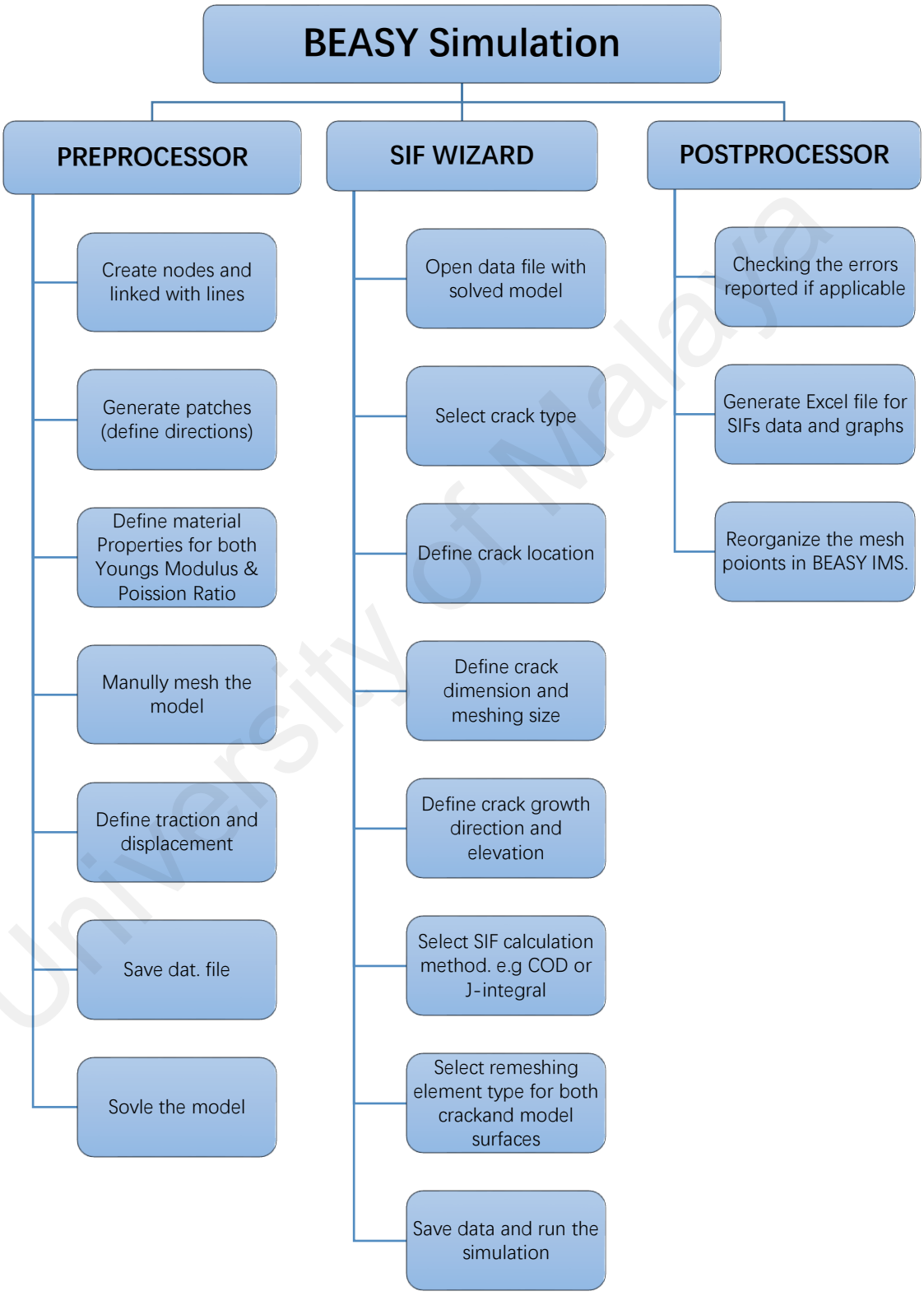

Figure 3.2: Steps to evaluate SIFs using BEASY

3.3.2.1 Model generation

As we can see from Figure 3.3, the square prismatic model consists of two zones which are the main square bar part where the embedded crack will be set inside of it and a short cylinder part where the torsion loading will be easily applied on it. In BEASY interface, the model below as a sample should be built with nodes firstly, then linked every node created before with straight lines for the prismatic bar part and with the circular arch lines for the cylinder.

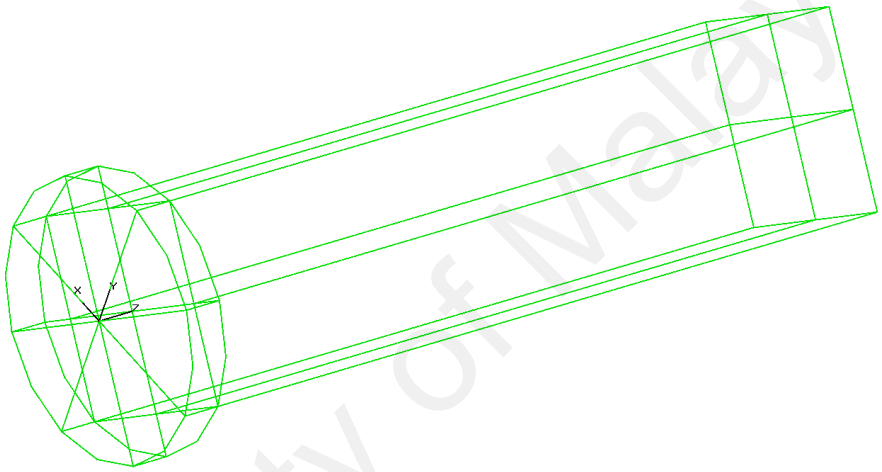

Figure 3.3: Points and lines generation in BEASY interface

After the last step is done, the patches with certain inward or outward direction should be created to cover the whole model. Mostly, each patch has been defined by 4 points created before, and for this work, there are totally 38 patches where they all connected together to cover the square prismatic bar. Also, each patch has the inward or outward definition with different color showed in the interface in BEASY, in Figure 3.4, the patches we can see are all marked in blue color which meant the outward direction.

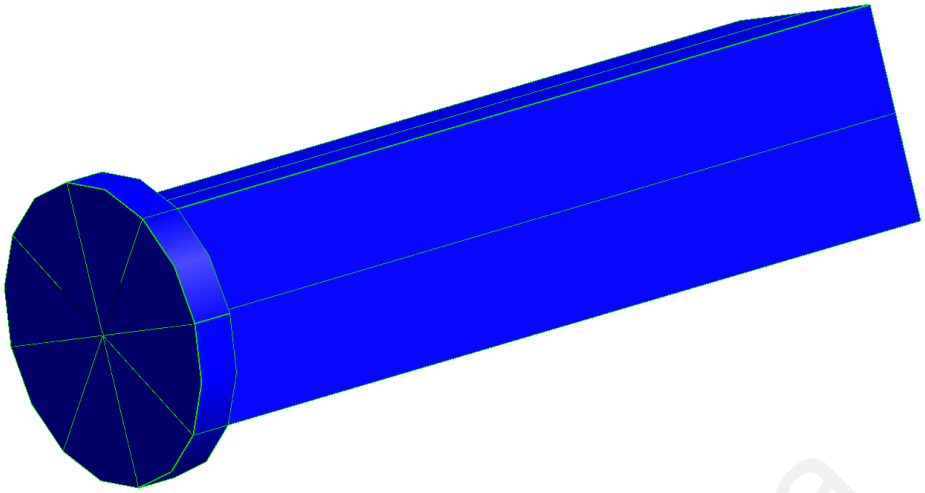

Figure 3.4: Patches generation in BEASY interface

3.3.2.2 Model meshing process

For two dimensional meshing process, BEASY applies elements to the boundaries. Either straight lines or curve lines could be the meshing lines. The number of nodes correlated to the element are shown in the Table 3.1, and the type of meshing lines are shown in Figure 3.5 below.

Table 3.1: 2D elements type in BEASY

Element Order	Number of Mesh Points	Number of Nodes
Constant	3	1
Linear	3	2
Quadrant	3	3

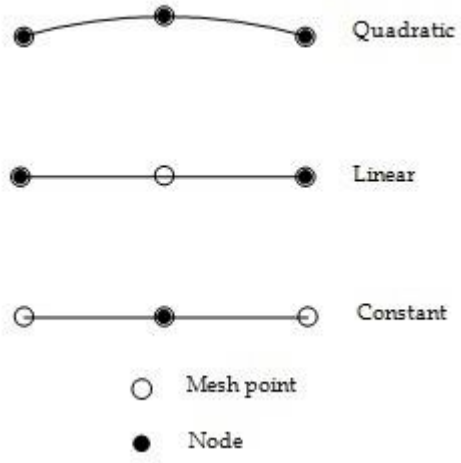

Figure 3.5: 2D line meshing lines in BEASY

For the three dimensional problems, BEASY applies elements to the patches. These patches types are either quadrilateral or triangular. There are nine mesh points for the quadrilateral elements, and six mesh points for the triangular. Number of nodes correlated to elements showed in Table 3.2 and 3.3. The illustrations of the element types showed in Figure 3.6.

Table 3.2: 3D quadrilateral elements type in BEASY

Element Order	Number of mesh points	Number of nodes
Constant	9	1
Linear	9	4
Reduced Quadratic	9	8
Quadratic	9	9

Table 3.3: 3D Triangular elements type in BEASY

Element Order	Number of mesh points	Number of nodes
Constant	6	1
Linear	6	3
Quadratic	6	6

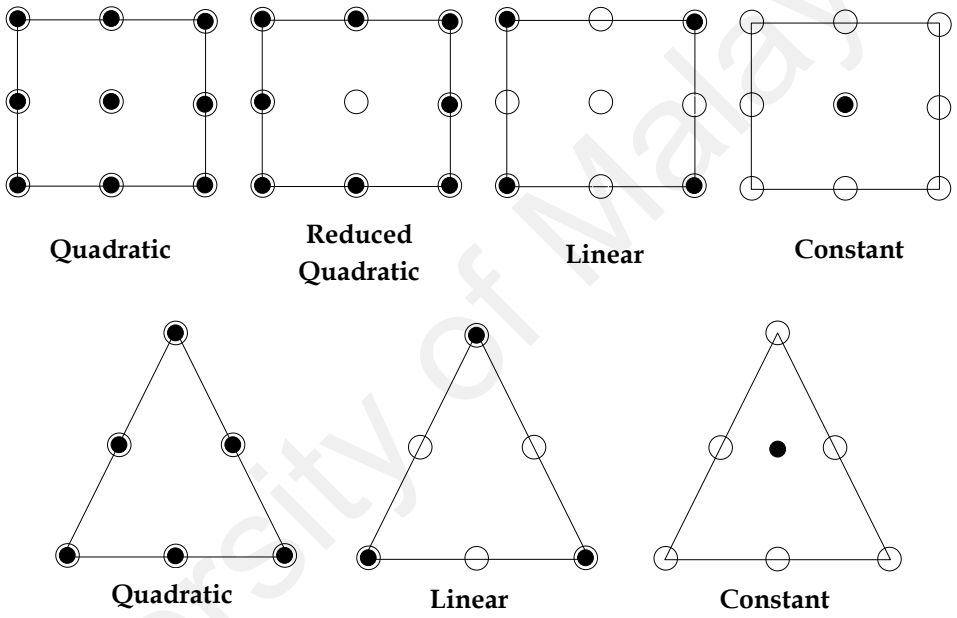

Figure 3.6: 3D elements type for quadrilateral and triangular patches meshing

In this work, all the patches of the model applied quadrilateral quadratic element meshes which were considerably accurate to simulate. There are total 16 fan shape elements on the surface of the left side of the end of the prismatic bar, and total 80 rectangular shape elements on the rectangular bar of the right side. After meshing process, the square prismatic bar model is shown in Figure 3.7.

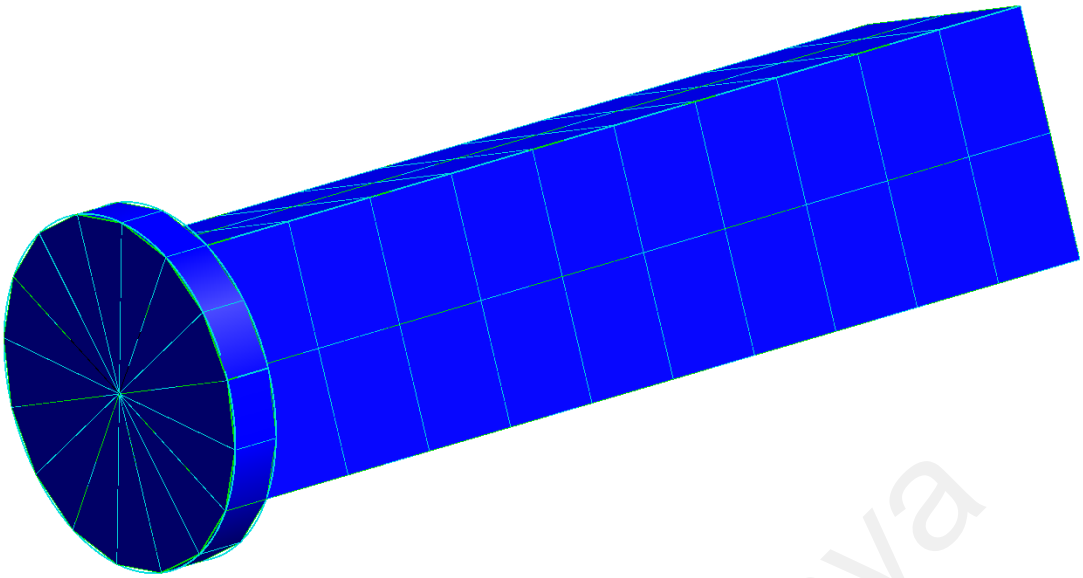

Figure 3.7: Element meshing of the model in BEASY interface

3.3.2.3 Boundary conditions

General speaking, boundary conditions can be applied with stress boundary conditions like traction, spring loads, constraints and so on, and potential boundary conditions could be heat transfer rate, flux density and thermal load, etc.

For the fracture mechanics study here, only stress boundary conditions are considered such as tension, torsion and displacements etc. The model with applied boundary condition is shown in Figure 3.8. As we can see here, the left end of the prismatic bar has been applied the torsion loading as one traction boundary condition, the other side has been applied current displacement constraint which is same as clamped constraint.

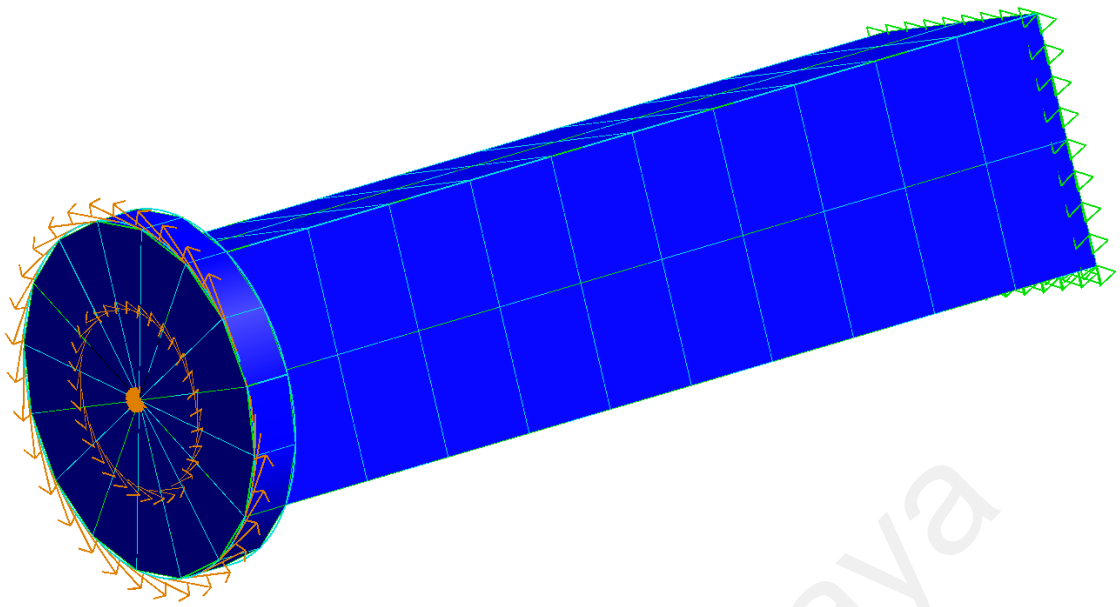

Figure 3.8: Model with applied boundary conditions in BEASY interface

3.3.2.4 Crack defining process

There is an independent calculation part called “SIF wizard” of BEASY to solve the SIFs with certain types of cracks subjected to cyclic loading that showed in Figure 3.9. Firstly, the model built before should be loaded in this wizard. Secondly, the model loaded here should also be checked and saved in a proper location to confirm there would not be any small mistake and the solved result could be found easily after all the procedure is done. Then the work process will be going to the step named “edit the crack simulation data” showed in the figure below.

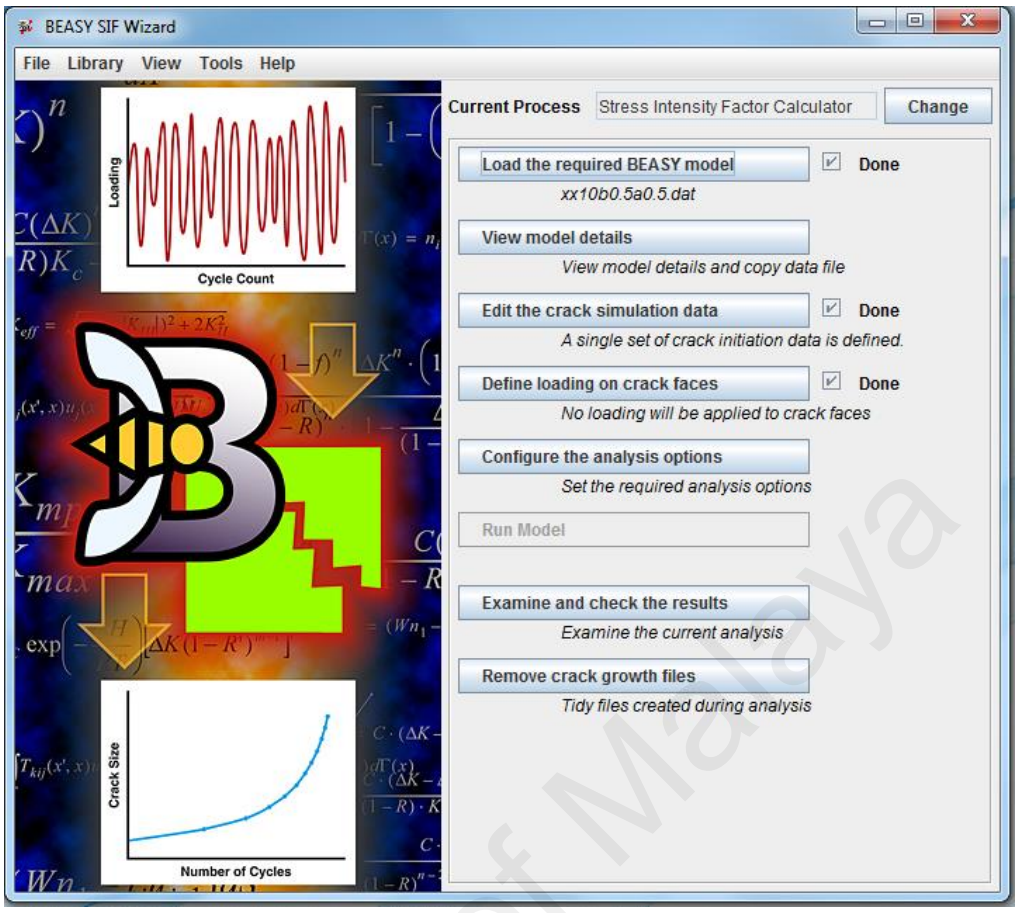

Figure 3.9: BEASY SIF wizard interface

After open the SIF wizard above, the first step to define the crack is choosing the number and the type of it as Figure 3.10 showed below. As the figure showed, the required type of analysis to be performed should be the simulation of a single crack in Figure 3.10 (a); next, this single crack should be defined as a 3D embedded elliptical crack expect the aspect ratio equal to one, then that would be a 3D embedded penny crack showed in Figure 3.10 (b).

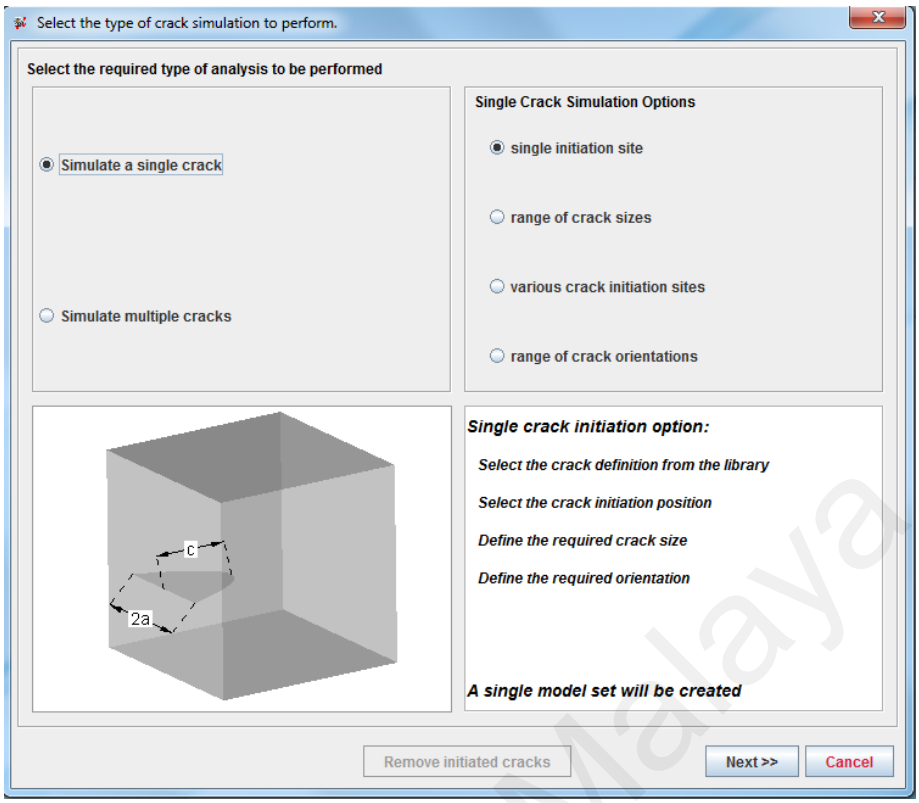

(a)

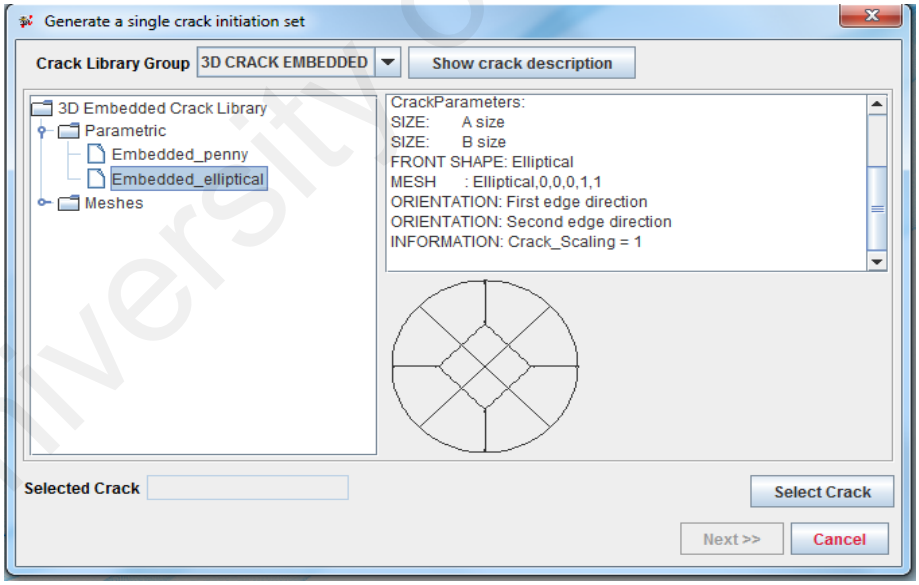

(b)

Figure 3.10: (a) crack quantity defining; (b) crack type defining

3.3.2.5 Defining the parameter of crack

There are totally 3 coordinates for the crack that should be defined in the Cartesian coordinate system in BEASY to accurately set an embedded elliptical crack. To describe the parameters of the crack clearly, Figure 3.11 illustrated these parameters clearly, crack initiation point is the center of the crack from where the crack starts to grow. The lengths of major and minor axes are *a* and *b* respectively. The direction of first crack edge to the second edge defines the way along the crack front in which the crack will grow. After the center of the crack location and the first crack edge direction defined, the second crack edge direction will determine the inclination of the embedded crack.

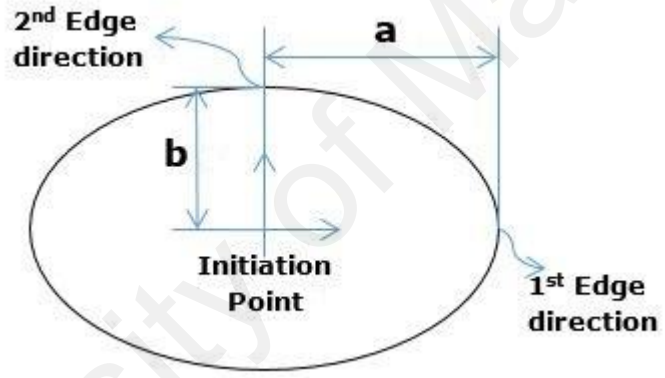

Figure 3.11: Parameters of embedded elliptical crack

The steps to define these parameters in SIF wizard are illustrated in the Figure 3.12. Firstly, the center of the embedded crack location inside of the model is defined as in Figure 3.12(a) where the first column represents the number of the crack and the second column defines the space rectangular coordinates. Next is to define the crack size parameters for both the length of major and minor axes as Figure 3.12(b). Then to define the orientation of the crack front where the crack will start to grow which is also called direction of first crack edge that the software could recognize in the first column in Figure 3.12(c), then the crack elevation in the second column is exactly the second edge direction in Figure 3.11.

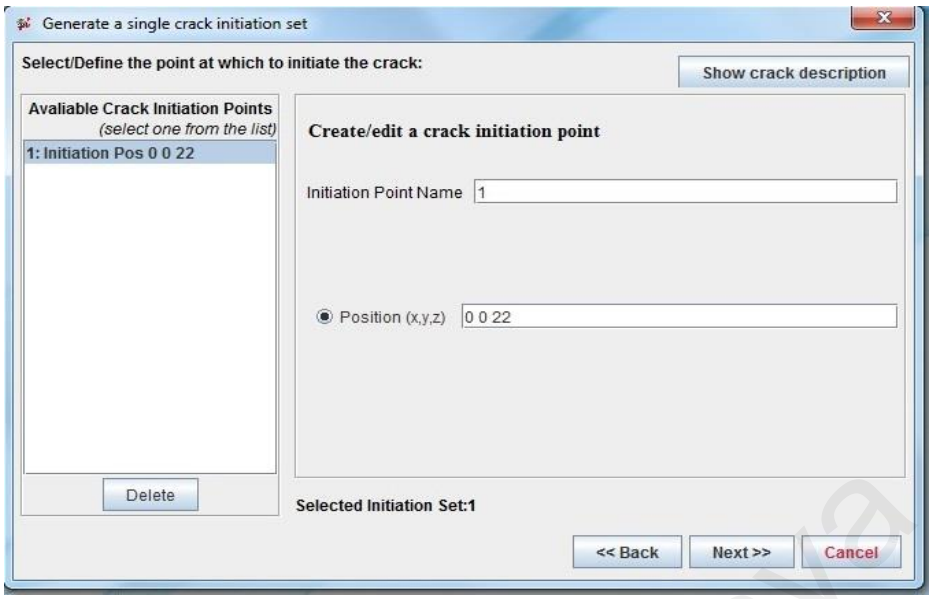

(a)

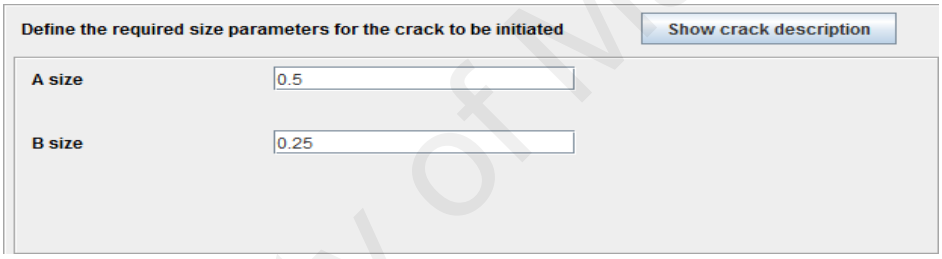

(b)

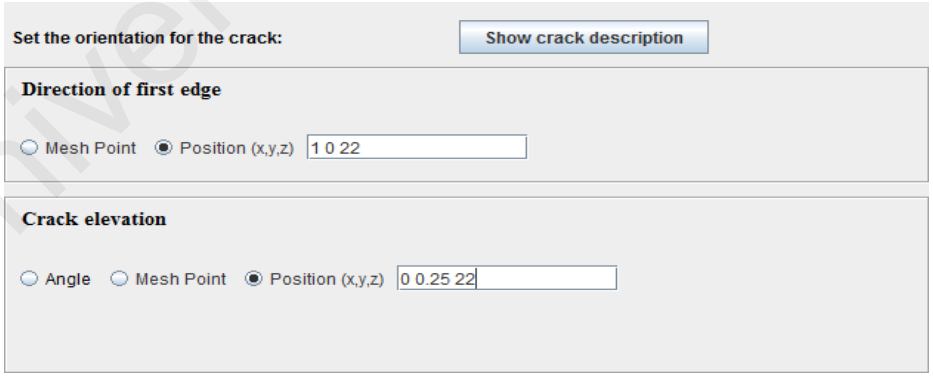

(c)

Figure 3.12: Steps to introduce Crack using BEASY SIF wizard (a) crack center point; (b) Crack size parameter; (c) crack growth direction & crack elevation parameter

3.3.2.6 Analysis method of SIFs

Stress intensity factors can be calculated in two options in BEASY, one is *J*-integral method, the other is crack opening displacement method (COD) as Figure 3.13 showed. Due to the more accurate results of it, *J*-integral method developed by Rice (1968) is more widely used by researcher and also has been chosen for this work.

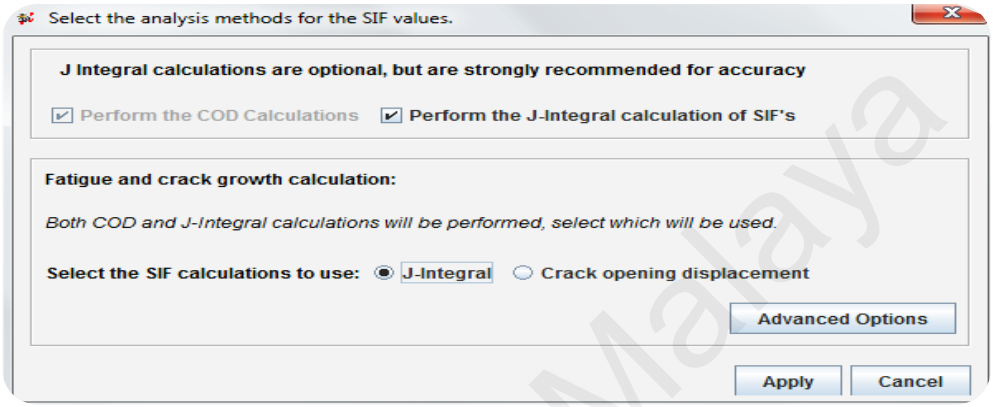

Figure 3.13: SIFs calculation method options in BEASY

J-integral is usually defined for non-elastic materials. It is known as a way to calculate the strain energy release rate, or energy per unit in a material for the fracture surface area. In the preceding calculations, we assume a monotonically loaded plastic material with the restriction that unloading is not permitted.

Rice (1968) recognized that for non-linear elastic, homogenous, isotropic body in static equilibrium a certain integral called J-integral along a closed path is always equal to 0. Now let Φ be a closed contour bounding a region 'A' occupied by the body as shown in Figure 3.14. Let x_1 and x_2 be the fixed coordinates to which all the coordinates are referenced. The J-integral is given by the equation

$$J_\phi = \oint_\phi \left(Wn_1 - \mathbf{T} \cdot \frac{\partial \boldsymbol{u}}{\partial x_1} \right) ds \tag{3.4}$$

Where W is strain energy density. The infinitesimal strain energy density dW is the work per unit volume done by the stress σ_{ij} during an infinitesimal strain increment dε_{ij}.

$$W = \int_0^{\varepsilon_{ij}} \sigma_{ij} d\varepsilon_{ij} \tag{3.5}$$

$$\sigma_{ij} = \frac{\partial W}{\partial \varepsilon_{ij}} \tag{3.6}$$

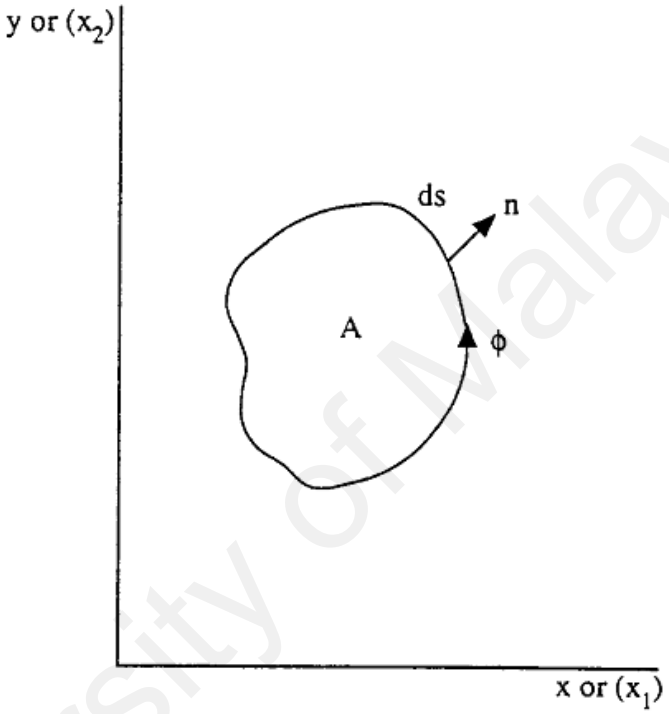

Figure 3.14: A counter clockwise closed contour, *Φ*

Also the traction vector **T** is a force per unit area acting on some plane in a stressed material and is defined according to the outward normal **n** to the contour *Φ*. **u** is a displacement vector. So

$$T_i = \sigma_{ij} n_j \tag{3.7}$$

$$\mathbf{u} = u_1 \mathbf{i} + u_2 \mathbf{j} \tag{3.8}$$

3.3.2.7 Element Selection

Selecting of the element type to mesh the crack and the surfaces in BEASY is shown in Figure 3.15. Hereby, In order to calculate SIFs in an efficient and accurate way, the element type on surface mesh is linear to make the calculation fast while the element type on crack is quadratic which is considered as a highly accurate method to proceed the calculation for the crack.

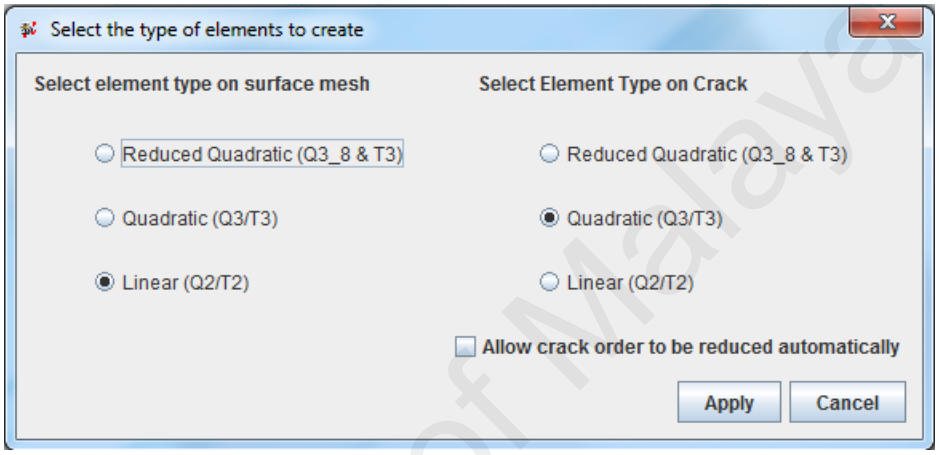

Figure 3.15: Element type selection for meshing the crack and the surfaces

3.3.2.8 Rest steps

At the end, BEASY saves the defined data for all the geometry of the model and crack, as well as the boundary conditions, then runs the simulation to calculate SIFs and finally carry out all three modes K_1, K_2 and K_3. The final results in Excel file in form of data values and graphs.

3.4 Summary

In this methodology chapter, the steps for using BEASY software and how it works to carry out the stress intensity factor values are reported in details. As well, the model property and crack parameters are illustrated. In next chapter, the few conclusions for the theory of elasticity, the effects of the crack aspect ratio, the effects of crack eccentricity

and the effects of crack inclination on the SIFs of an embedded crack in a square prismatic bar under torsion loading are presented and discussed.

CHAPTER 4

RESULTS & DISCUSSIONS

4.1 Introduction

In this chapter, firstly, the benchmarking for the BEASY software has been done and compared with Newman-Raju solution (Newman Jr & Raju, 1986). Secondly, several results for elasticity have been concluded which could be considered as the theoretical principal and explanation for the SIFs effects of different parameters of embedded crack. Afterward, stress intensity factor results have been presented for an embedded crack with different parameters in square prismatic bars under torsion loading. Lastly, a comparison between different geometries of models have been showed and concluded.

The parameters and notations used for the model are depicted in Figure 4.1. Embedded cracks with fixed b = 0.5 mm and aspect ratio of *b/a* are introduced in the square bar. The characteristic mesh size for crack front discretization for all cracks studied is approximately 0.02 mm, and all SIFs are normalized by $K_0 = \tau_{\max}\sqrt{\pi b}$, where $\tau_{\max} = 100$ MPa. BEASY software, Boundary element based, is emerging software to solve boundary value problems in various engineering fields. To fulfill the objectives of this research, simulations are carried out using BEASY software. To demonstrate the accuracy of BEASY software, benchmarking is carried out by comparing BEASY results with the available results in literature.

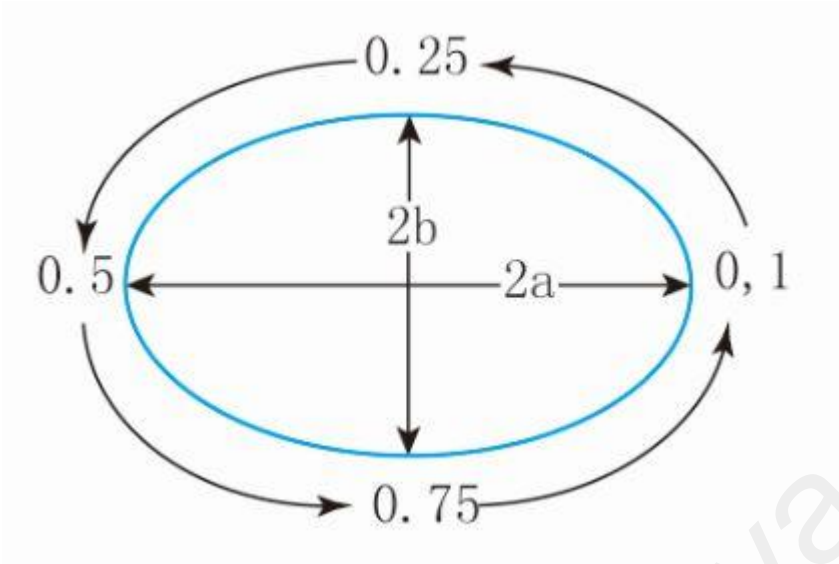

Figure 4.1: Parameters and normalized position along crack front

4.2 Benchmarking

Since no solution for torsionally loaded prismatic bar with embedded cracks is available, Newman-Raju (NR) solution (Newman Jr & Raju, 1986) for embedded elliptical crack in a square bar loaded normally is used instead to benchmark the results of BEASY. A 20 × 20 mm^2 benchmarking model with 80 mm length is designed to validate the BEASY software. In Figure 4.2, we present the results of K_1 for aspect ratios b/a = 0.5, 1, and 2 subjected to normal stress of 100 MPa.

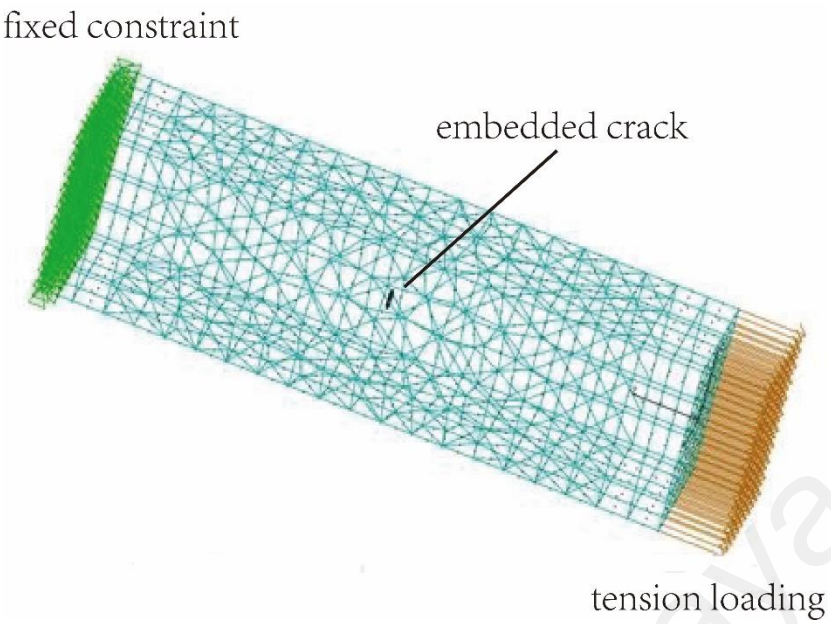

Figure 4.2: Benchmarking model with an embedded crack

This simulation has characteristic mesh size of 0.05 mm on the crack front. Good agreement is observed the results overlap each other for most part, and there is a small difference for maximum values albeit that for minimum seems to be sizable. We remark that NR closed-form solution is approximate as it showed in Figure 4.3 below.

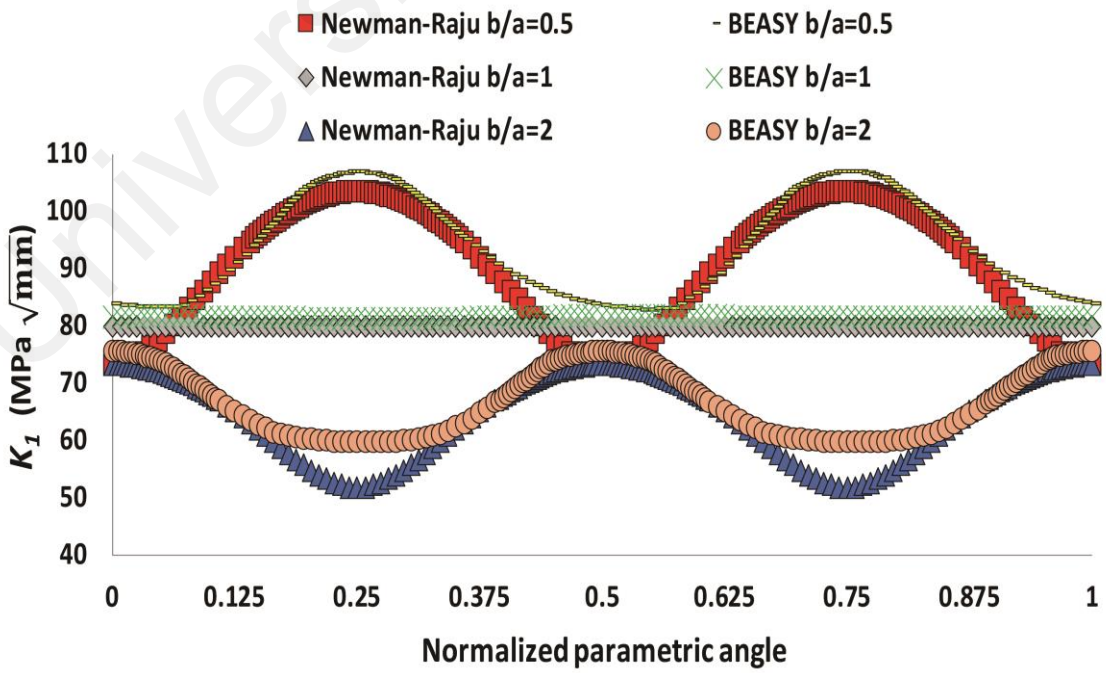

Figure 4.3: K_1 due to tensile loading on an embedded elliptical crack with aspect ratios b/a = 0.5, 1, and 2 within a square bar

4.3 Results from elasticity

Rectangular bar is a straightforward geometry, yet the result of the shear stress is still lengthy since a second order partial differential equation must be fathomed. To start, the equation that models all torsional shear stress is,

$$\frac{\partial^2 \varphi}{\partial x^2} + \frac{\partial^2 \varphi}{\partial y^2} = -2G\theta \tag{4.1}$$

where G is the shear modulus, θ is the angle (radians) of twist per unit length (not the total twist) and φ is the scalar stress function (used to discover shear stress).

In our case the maximum torsional shear stress has been defined as $\tau_{max} = 100$ MPa, and as the square bar geometry setting above, the torque could be calculated as M = 20.8 Nm since the width 2A and height 2B both equal to 10 mm as the Figure 4.4(a) showed below. There are two axes (X and X') on the cross section for studying how the shear stress variate along them.

Timoshenko and Goodier (1970) has given the relationship between the torque M and the angle (radians) of twist per unit length θ,

$$M = 0.1406G\theta(2A)^4 \tag{4.2}$$

So, $\theta = 70446.39$ rad.

The dimension of "A" and "B" are diverse for the time being, so the derived solution can be utilized for any rectangular bar. The utilization of the x-axis facing the right is steady with standard beam coordinates (z is along the bar center, or coming out of the page for this case). The torsional shear stresses in the rectangular bar is not at all like a round bar, the stresses will change for diverse area around the middle. This makes the solution troublesome (and protracted).

Like all solutions to differential equations, a trial solution is proposed, and afterward substituted back into locate a particular solution. Since the solution ought to be symmetrical around both the *x*-axis and *y*-axis, a cos function ought to work.

As a beginning stage, expect the stress function, φ, is

$$\sum_{n=1,3,5..}^{\infty} B_n \cos\frac{n\pi x}{2A} Y_n, \tag{4.3}$$

where b_n are constants (will be counterbalanced later) and Y_n are functions of "*y*" that are not yet set. Presently, substitute this expected solution once more into the differential equation, giving

$$\left[\sum B_n \left(-\frac{n^2\pi^2}{4A^2}\right)\cos\frac{n\pi x}{2A} Y_n\right] + \sum B_n \cos\frac{n\pi x}{2A} Y_n'' = -2G\theta, \tag{4.4}$$

Every one of the terms on the left have cosine functions, yet the right hand side does not. To make all terms steady, the -2$G\theta$ consistent term can be composed as a fourier series (fundamentally only a series utilizing sine and cosine) as

$$2G\theta = \sum_{n=1,3,5..}^{\infty} 2G\theta \frac{4}{n\pi}(-1)^{(n-1)/2}\cos\frac{n\pi x}{2A}, \tag{4.5}$$

This may appear to be complex, but it will work out at last. On the off chance that the 2$G\theta$ series is substituted into the past mathematical equation, the cos terms will scratch off, giving

$$\left[\sum b_n \left(-\frac{n^2\pi^2}{4A^2}\right) Y_n\right] + \sum B_n Y_n'' = -\sum 2G\theta \frac{4}{n\pi}(-1)^{(n-1)/2}, \tag{4.6}$$

Where the " (prime) marks speak to derivatives as for *y*. Adjusting, moving b_n term to the right hand side, and dropping the summation symbol for effortlessness (as yet summing on all terms with n), giving

$$Y_n'' - \frac{n^2\pi^2}{4A^2} Y_n = -2G\theta \frac{4}{n\pi B_n}(-1)^{(n-1)/2}, \tag{4.7}$$

The Y_n expressions are elements of *y* that have not been set yet. It will be done at this point. Fundamentally, the equation above is another differential equation. The general result is

$$Y_n = a_0 \sinh\frac{n\pi y}{2A} + b_0 \cosh\frac{n\pi y}{2A} + 2G\theta\frac{16A^2}{n^3\pi^3 B_n}(-1)^{(n-1)/2}, \quad (4.8)$$

Presently the boundary conditions can be connected to decide the constants A and B. To start with, since the result will be symmetrical about the x-axis, there can be no sinh term (anti symmetric). Along these lines A absolutely will be zero. Next, B can be found with the boundary conditions $\varphi = 0$ at the edge, or when $y = \pm b$, giving

$$b_0 = \frac{2G\theta\frac{16A^2}{n^3\pi^3 B_n}(-1)^{(n-1)/2}}{\cosh\frac{n\pi B}{2A}}, \quad (4.9)$$

This give Y_n as

$$Y_n = 2G\theta\frac{16A^2}{n^3\pi^3 B_n}(-1)^{(n-1)/2}\left[1 - \frac{\cosh\frac{n\pi y}{2A}}{\cosh\frac{n\pi B}{2A}}\right], \quad (4.10)$$

Substituting Y_n, back into the stress function, φ, gives

$$\varphi = \sum_{n=1,3,5..}^{\infty} G\theta\frac{32A^2}{n^3\pi^3}(-1)^{\frac{(n-1)}{2}}\left[1 - \frac{\cosh\frac{n\pi y}{2A}}{\cosh\frac{n\pi B}{2A}}\right]\cos\frac{n\pi x}{2A}, \quad (4.11)$$

This is the full answer for the stress function any location (*x*, *y*) for a rectangular intersection. Taking a derivative to *x* could discover the shear stress on the *y*-*z* plane, giving

$$\tau_{yz} = -\frac{\partial y}{\partial x} = G\theta\frac{16A}{\pi^2}\sum_{n=1,3,5..}^{\infty}\frac{1}{n^2}(-1)^{(n-1)/2}\left[1 - \frac{cosh\frac{n\pi y}{2A}}{cosh\frac{n\pi B}{2A}}\right]sin\frac{n\pi x}{2A} \quad (4.12)$$

In like manner, the stress in the *x*-*z* plane can be found from

$$\tau_{xz} = \frac{\partial \varphi}{\partial y} = -G\theta \frac{16A}{\pi^2} \sum_{n=1,3,5..}^{\infty} \frac{1}{n^2} (-1)^{(n-1)/2} \left[\frac{sinh\frac{n\pi y}{2A} cos\frac{n\pi x}{2A}}{cosh\frac{n\pi B}{2A}} \right] \quad (4.13)$$

The overall shear stress will be a mix of both the *y*-*z* and *x*-*z* plane stress.

$$\tau_{xy} = \sqrt{\tau_{xz}^2 + \tau_{yz}^2} \quad (4.14)$$

Last but not least, the definition domain of the function above has been set from 1 to infinite, so we should also consider the convergence of it.

As the figure showed in Figure 4.4(b), the Equation (4.12) is going to converge when $n \geq 9$, so that the stress components for τ_{yz} could be accurately found based on the graphs above. Here, the normalized position on cross section respected to the length of the *a* along axis *X'* and the normalized stress utilized the function

$$\hat{\tau} = \tau / \tau_{max} \quad (4.15)$$

where the τ_{max} is the maximum shear stress applied on the square bar that is 100 MPa.

Likewise, the τ_{xz} in Figure 4.4(c) converged even more faster than the τ_{yz}, in which the graphs showed that this function converged when $n \geq 9$. Then followed the Equation (4.14), Figure 4.4(d) shows the shear stress distributions along *X* and *X'*, these results would be useful to understand the behavior of SIFs for cracks with offsets from the centroid.

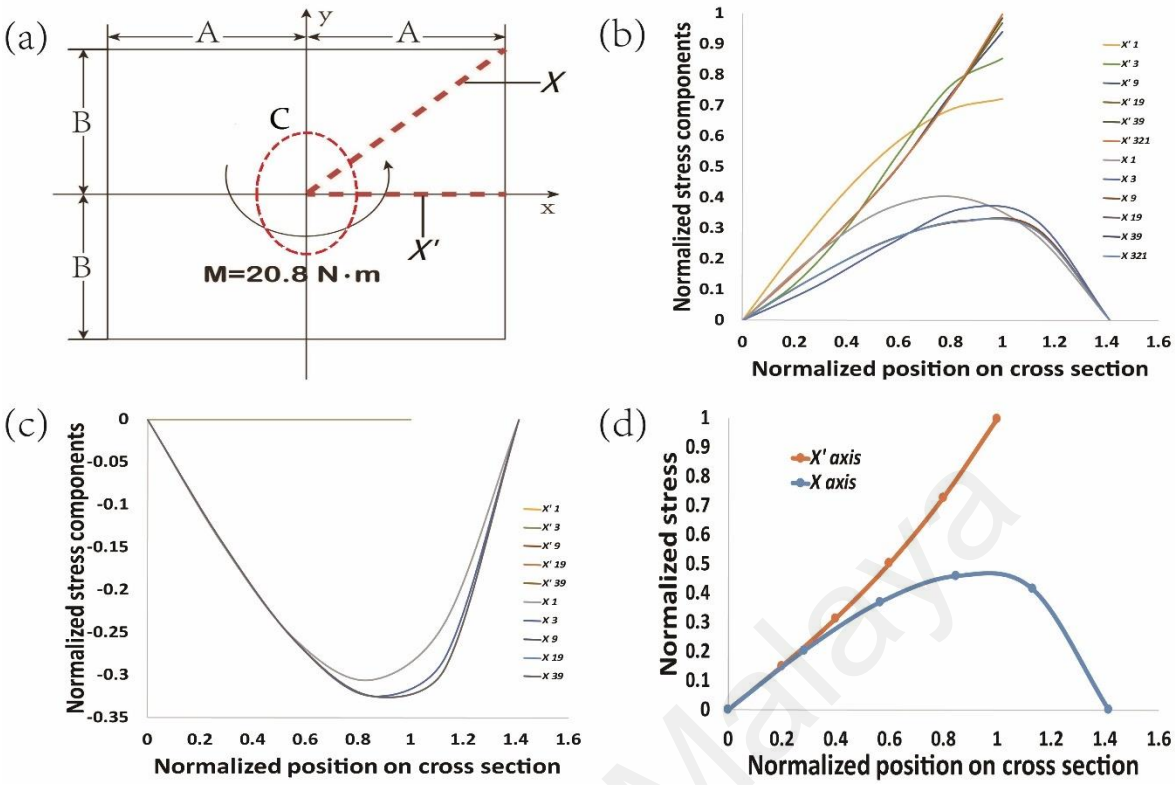

Figure 4.4: (a) The geometry of a rectangular bar; (b) The convergence of normalized τ_{yz}; (c) The convergence of normalized τ_{xz}; (d) shear stress distributions

Along an elliptical contour of *C* as showed in Figure 4.4(a) parametrized by

$$(x, y) = (a\cos t, b\sin t) \tag{4.16}$$

the tangent and normal vectors can be written as

$$\mathbf{e}_n = \left(1, \frac{a}{b}\tan t\right) \Big/ \sqrt{1 + \frac{a^2}{b^2}\tan^2 t} \tag{4.17}$$

And

$$\mathbf{e}_t = \left(-\frac{a}{b}\tan t, 1\right) \Big/ \sqrt{1 + \frac{a^2}{b^2}\tan^2 t} \tag{4.18}$$

respectively; and this allows for the calculation of the normal and tangential shear component respectively as

$$\tau_n = \left(\tau_{xz}, \tau_{yz}\right) \cdot \mathbf{e}_n \tag{4.19}$$

And

$$\tau_t = \left(\tau_{xz}, \tau_{yz}\right) \cdot \mathbf{e}_t. \tag{4.20}$$

The distributions of these components, as depicted in Figure 4.5, may be used to guide our intuition about the in-plane and anti-plane SIFs of K_2 and K_3.

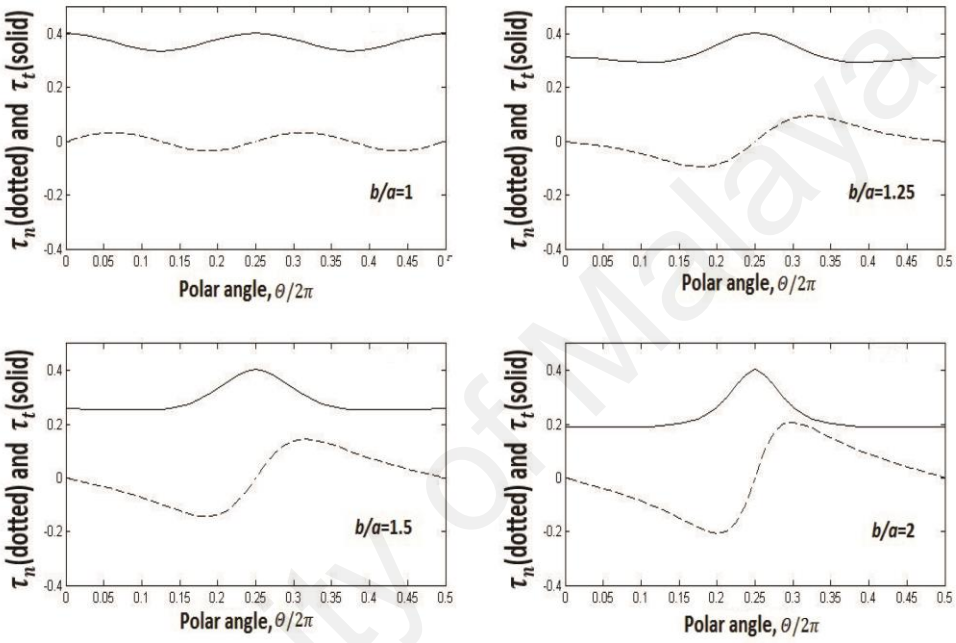

Figure 4.5: Distribution of the normal (dotted line) and tangential (solid line) shear stresses along an elliptical contour *C* around the centroid with vertical axis length *b* = 0.5 mm and aspect ratio *b/a* as indicated in the subplots

4.4 Center cracks of different aspect ratio

4.4.1 Introduction

Crack aspect ratio is the ratio between the major and minor axis of the elliptical crack as shown in the Figure 4.6, in this work, cracks with aspect ratio $\frac{b}{a} \in \{1, 1.25, 1.5, 1.75, 2\}$ and with b = 0.5 mm are studied.

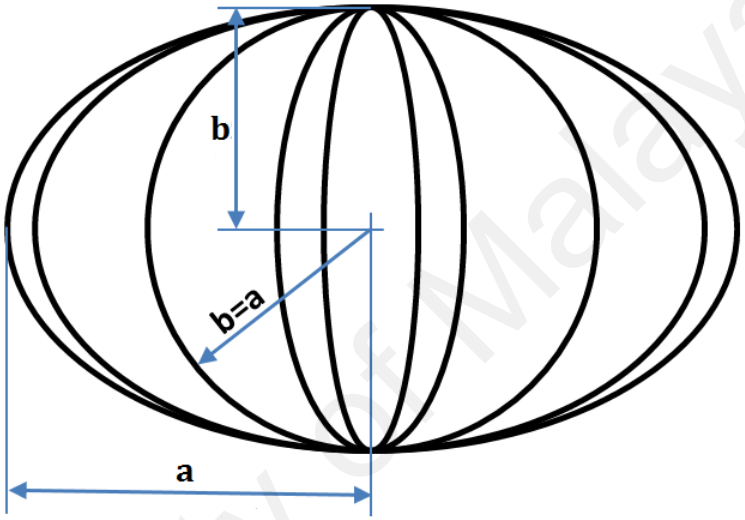

Figure 4.6: Circular and elliptical shapes different crack aspect ratios (b/a)

4.4.2 Effects of crack aspect ratio for center cracks

Figure 4.7(a) and Figure 4.7(b) depicted SIFs K_2 and K_3 for center cracks. K_1 is irrelevant as it would equal to zero for normally oriented cracks. For b/a = 1 (i.e. a penny crack), the in-plane sliding mode K_2 along the crack front for b/a = 1 is approximately zero, and the anti-plane tearing mode K_3 is uniform. These could be expected intuitively as the shear stress field without cracks appears to be nearly concentric circles for small radial distances away from the centroid. The two-fold symmetry of a penny crack about the centroid with respected to the loading results in the periodic behavior seen in Figure 4.7(a) and 4.7(b). As the crack becomes more elliptical, the maximum value of K_2 increases and K_3 decreases; and as intuitively expected by referencing Figure 4.5, it is seen to shift towards

the apical crack front positions of 1/4 and 3/4 for Mode II and stays at these apical positions for Mode III. The ratio of $0 \leq {K_2^{\max}}/{K_3^{\max}} < 1$, suggesting that the mild Mode III dominance is reduced as crack becomes more elliptical. As depicted in Figure 4.7(c) and (d), $K_2^{\max}$ is observed to be increasing at a slower rate for $b/a > 1.5$, while $K_3^{\max}$ decreases more or less linearly with b/a.

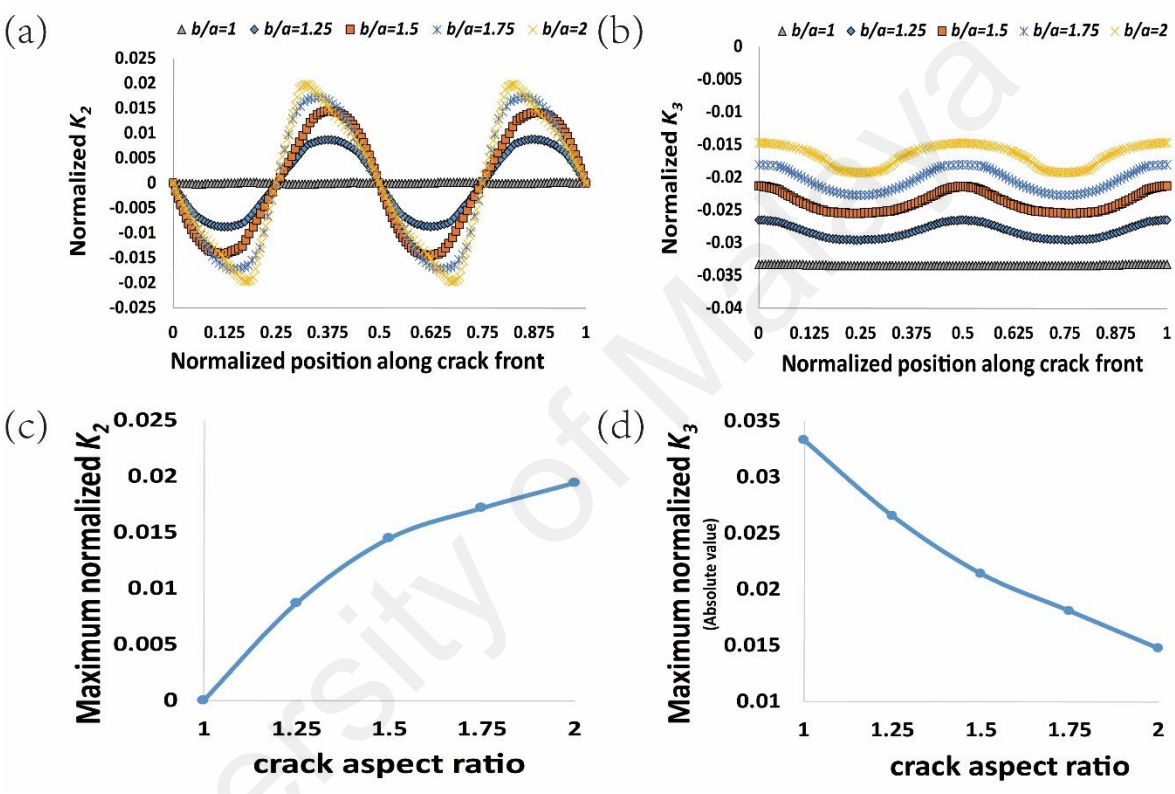

Figure 4.7: (a) K_2 for embedded center cracks with different aspect ratios (b = 0.5 mm); (b) K_3 for embedded center cracks with different aspect ratios (b = 0.5 mm); (c) $K_2^{\max}$; (d) $K_3^{\max}$.

4.5 Eccentric cracks

4.5.1 Introduction

We define the eccentricity e in the sense of an offset from the centroid as $e \cdot \frac{A}{5}$ = true distance from centroid, and sample these locations on X and X' (see Figure 4.8): (i) $e \in \{1, 2, 3, 4\}$ along X', and (ii) $e \in \{\sqrt{2}, 2\sqrt{2}, 3\sqrt{2}, 4\sqrt{2}\}$ along X. And the normalized position along crack front are showed for eccentric cracks along different axes.

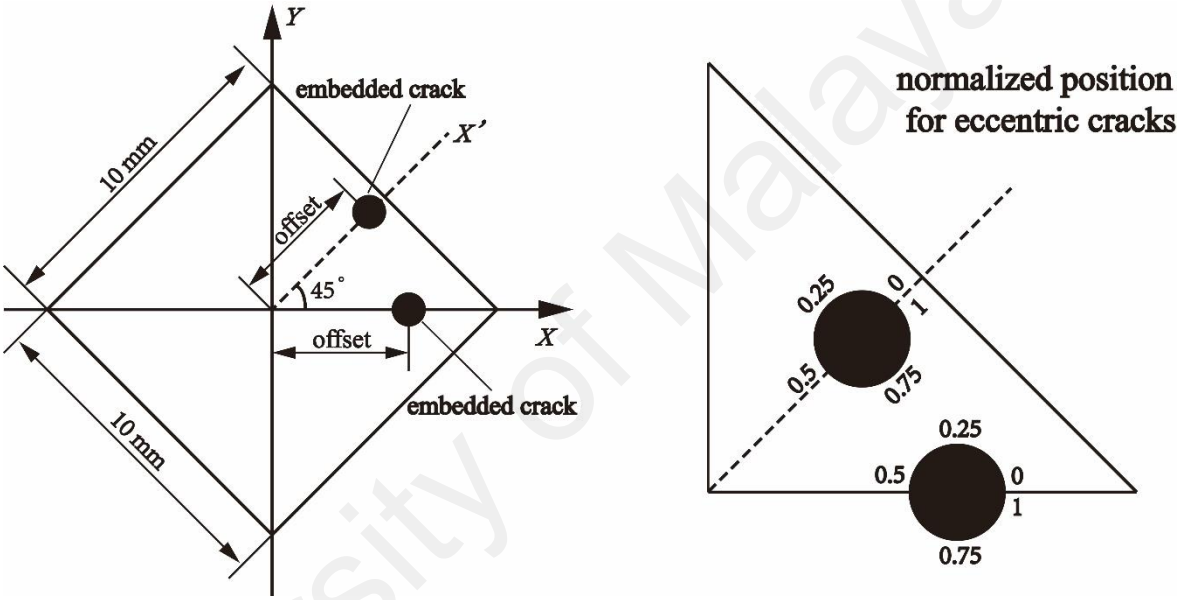

Figure 4.8: Eccentric embedded crack with aspect ratio *b/a* = 1 on the cross section of the square prismatic bar

4.5.2 Effects of eccentricity for penny cracks

Nearly symmetrical or anti-symmetrical profile about the major or minor elliptic axes is observed in Figure 4.9(a) to (d). $K_2^{\max}$ and $K_3^{\max}$ are found to be respectively at locations which are very close to the major and minor axes. The maximum SIFs as a function of the eccentricity, as depicted in Figure 4.9(e) to (f), are qualitatively similar to Figure 4.4(d); and for all cases, $K_2^{\max} > K_3^{\max}$ is observed.

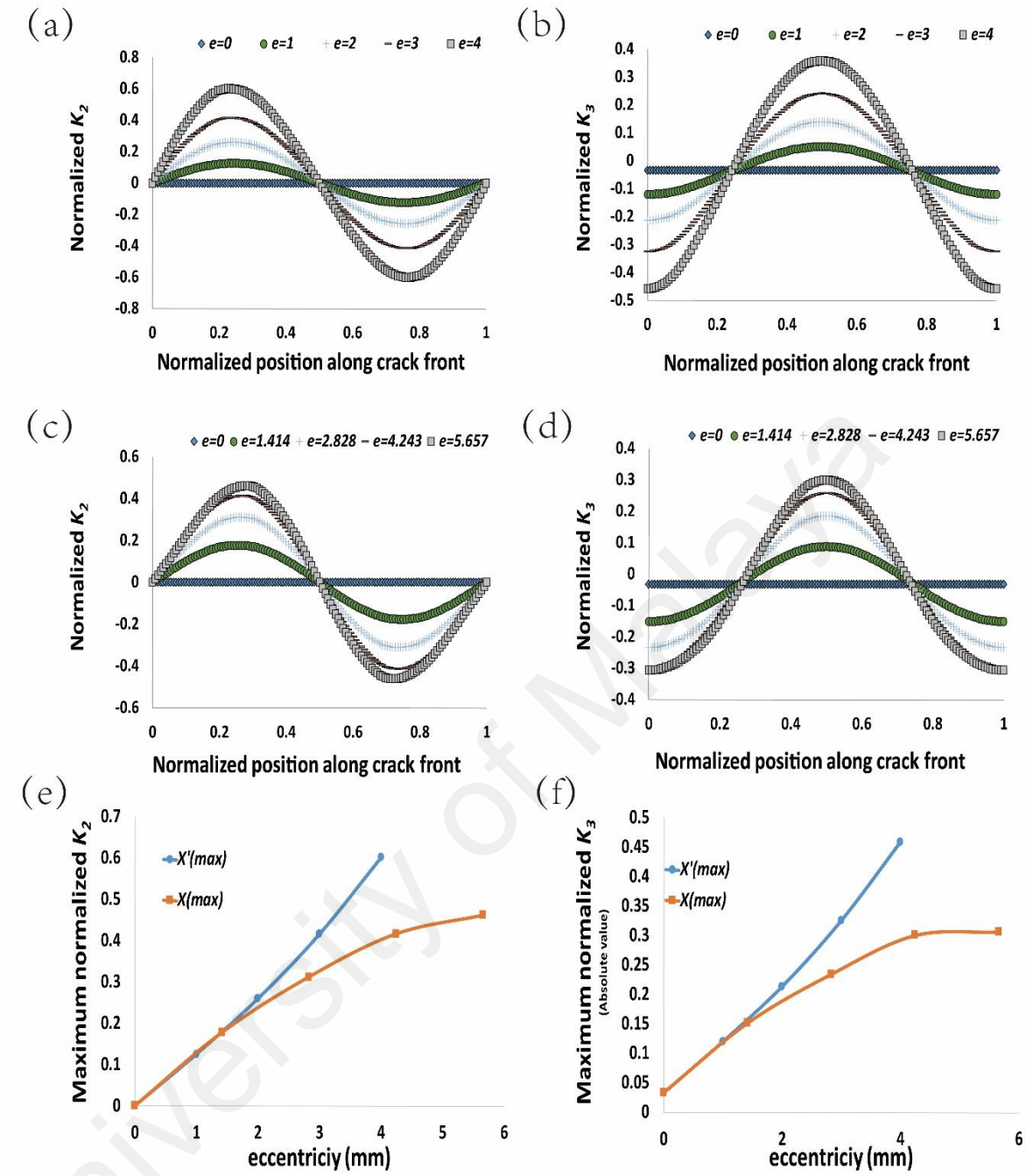

Figure 4.9: (a) K_2 of penny crack for different eccentricities along *X'* axis; (b) K_3 of penny crack for different eccentricities along *X'* axis; (c) K_2 of penny crack for different eccentricities along *X* axis; (d) K_3 of penny crack for different eccentricities along *X* axis; (e) $K_2^{\max}$; (f) $K_3^{\max}$

4.5.3 Effects of eccentricity for elliptical cracks

Last but not least, the eccentricity rules could be not only applied to the penny crack showed in this section but also to the elliptical crack $(b/a \neq 1)$. For example, $b / a = 2$, with $b = 0.5$ mm is shown in Figure 4.10. But since the size of the elliptical cracks became

smaller as a reduced from 0.5 mm to 0.25 mm, K_2 and K_3 in the same locations also showed smaller values compared with Figure 4.9 above.

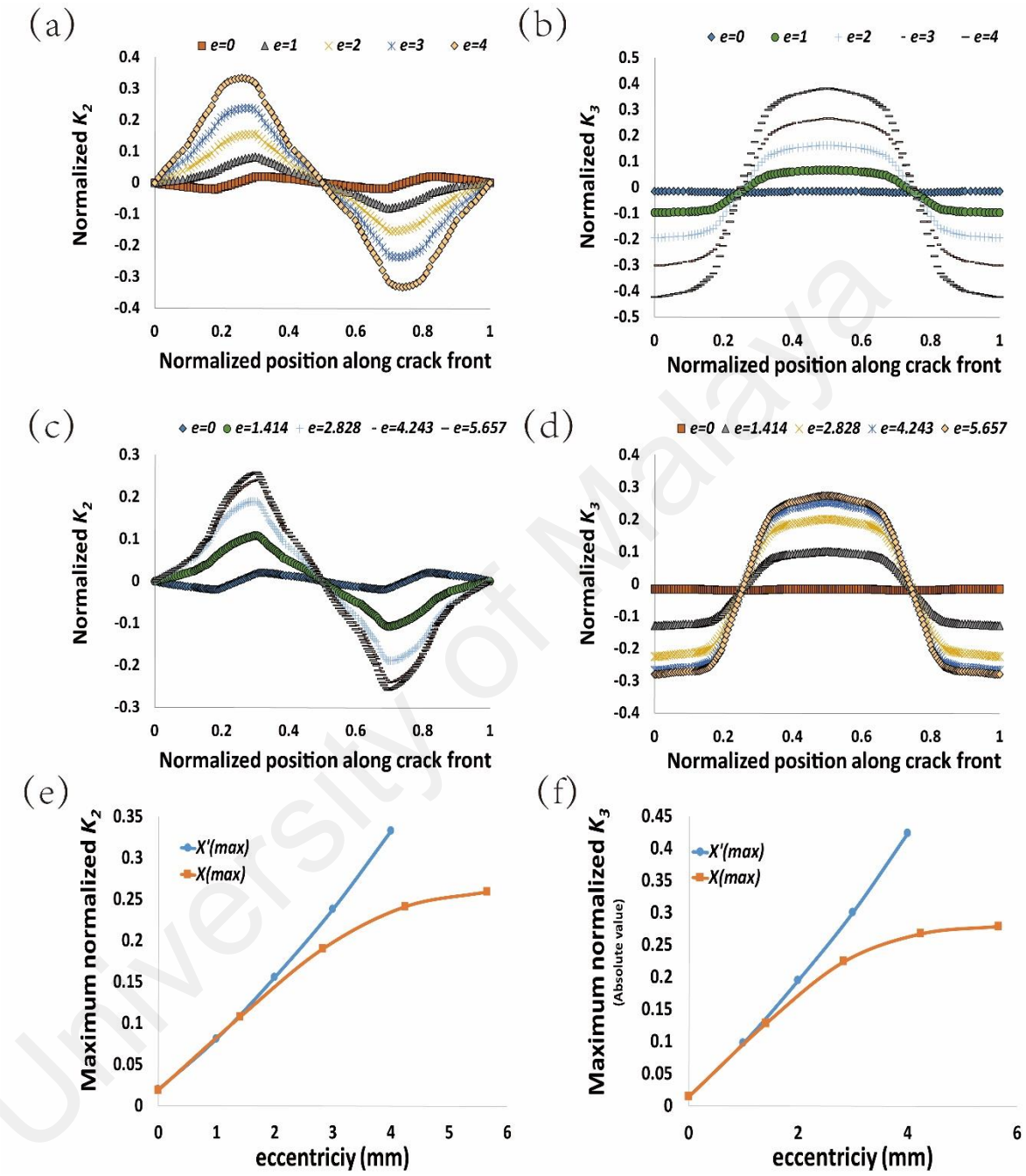

Figure 4.10: (a) K_2 of elliptical crack for different eccentricities along X' axis; (b) K_3 of elliptical crack for different eccentricities along X' axis; (c) K_2 of elliptical crack for different eccentricities along X axis; (d) K_3 of elliptical crack for different eccentricities along X axis; (e) $K_2^{\max}$; (f) $K_3^{\max}$

4.6 Cracks with inclination

4.6.1 Introduction

Crack inclination is the inclination from the crack plane. Angle α indicates the crack orientation which is considered from $0°$ to $90°$ to investigate its effects on stress intensity factor value as showed in Figure 4.11. We proceed to study cracks with inclination with respect to the normal plane of the prismatic axis of the bar. Inclinations of $\alpha \in \{0^{\circ}, 22.5^{\circ}, 45^{\circ}, 67.5^{\circ}, 90^{\circ}\}$ along *X'* axis (correlated to Figure 4.8) are introduced.

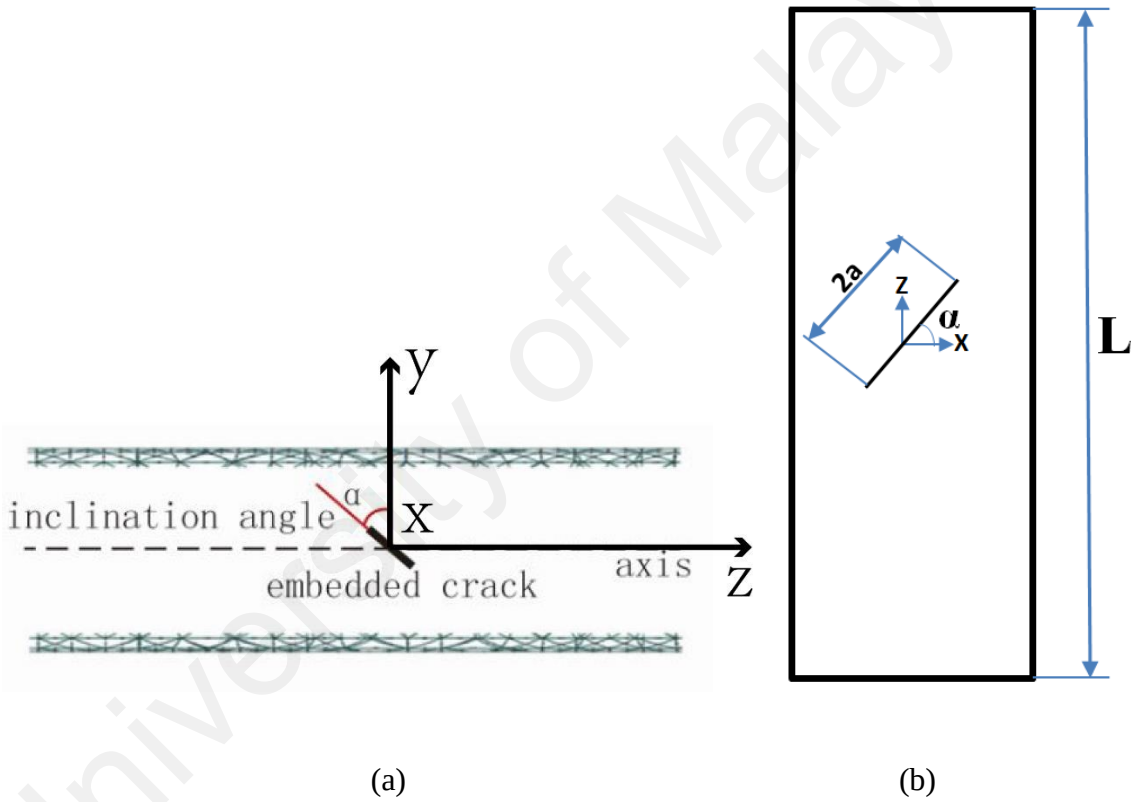

(a) (b)

Figure 4.11: (a) Crack inclination α from *y-z* plane; (b) Crack inclination α from *x-z* plane

4.6.2 Effects of inclination for penny cracks

The SIFs of embedded crack with inclinations would be even more complicated since the effect of α is a complex stress field that leads to all three modes of SIFs. Here, the size of penny crack is $b = a = 0.5$ mm. After observation, the most severe inclination for $K_1^{\max}$

is found to be $\alpha = 45^{\circ}$. $K_1^{\max}$ for all cases is located at the crack front position corresponding to the minor axis as shown in Figure 4.12(a-c). Figure 4.13 and Figure 4.14 show the SIFs respectively for K_2 and K_3. The most severe orientation for both modes is $\alpha = 90^{\circ}$. Interestingly, location for $K_3^{\max}$ is on the minor axis, different from that of non-inclined cracks; and the location of $K_2^{\max}$ remains unchanged.

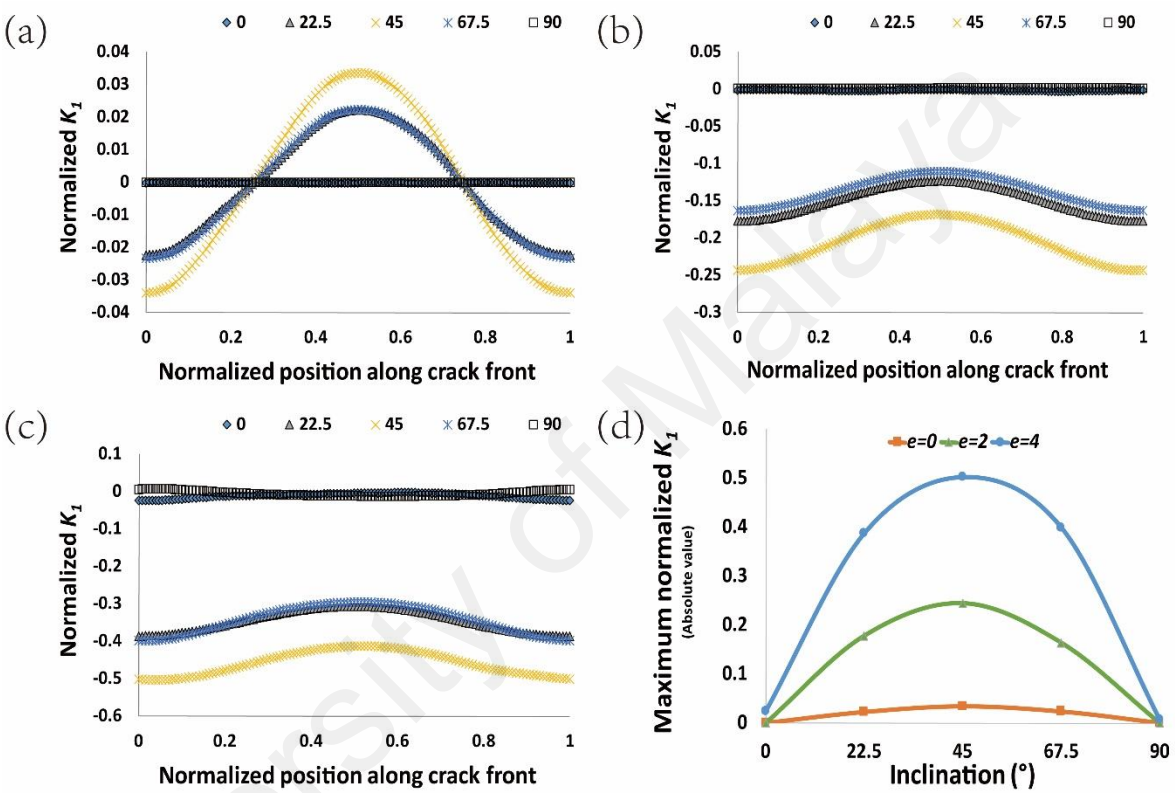

Figure 4.12: (a) K_1 of a center penny crack with inclinations; (b) K_1 of inclined penny cracks with e = 2 along X'; (c) K_1 of inclined penny cracks with e = 4 along X'; (d) $K_1^{\max}$ along X'.

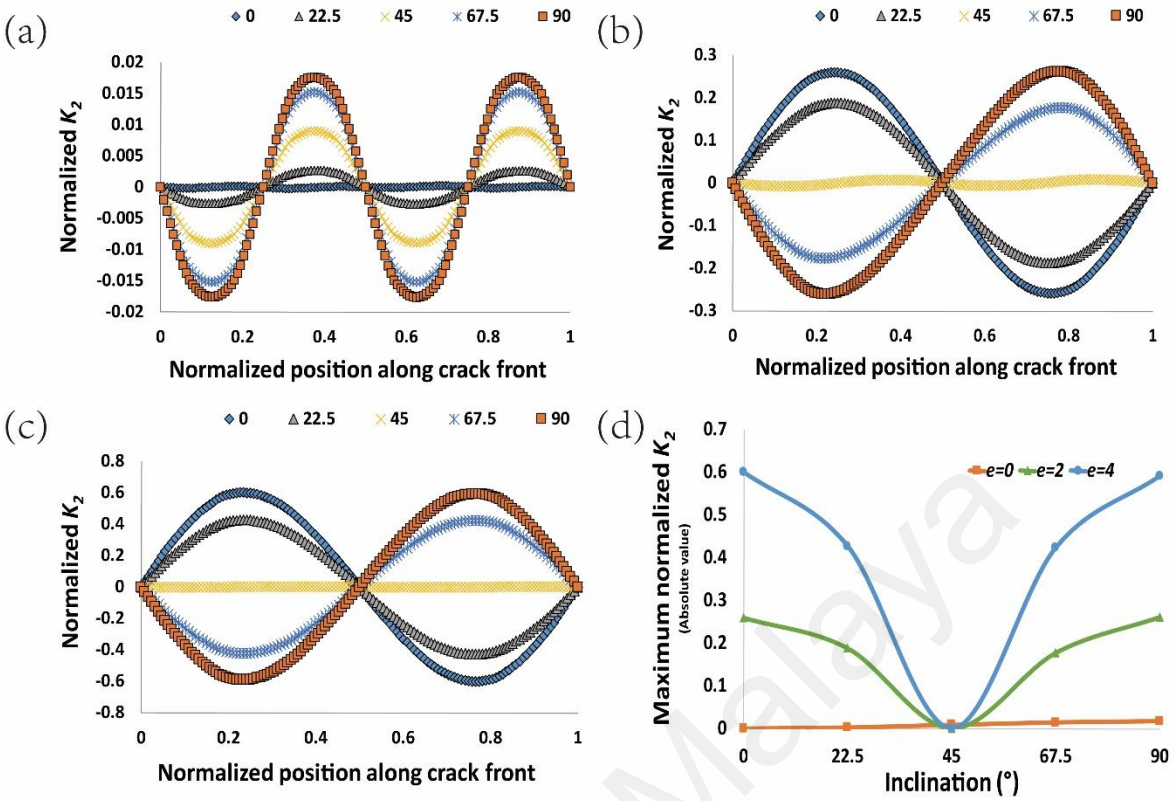

Figure 4.13: (a) K_2 of a center penny crack with inclinations; (b) K_2 of inclined penny cracks with e = 2 along X'; (c) K_2 of inclined penny cracks with e = 4 along X'; (d) $K_2^{\max}$ along X'.

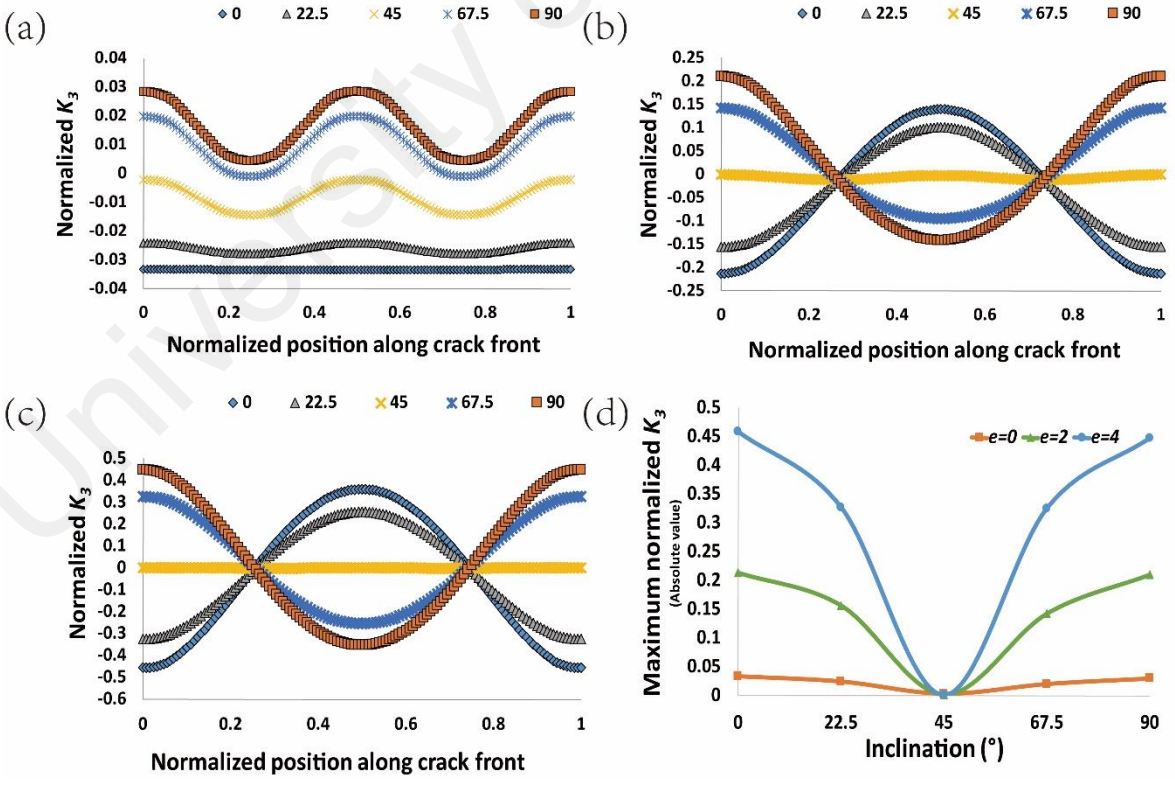

Figure 4.14: (a) K_3 of a center penny crack with inclinations; (b) K_3 of inclined penny cracks with e = 2 along X'; (c) K_3 of inclined penny cracks with e = 4 along X'; (d) $K_3^{\max}$ along X'.

4.6.3 Effects of inclination for elliptical cracks

As for the effects of inclination for elliptical cracks (here, b = 0.5 mm, a = 0.25 mm), all the findings for K_1 are the same with penny cracks above as showed in Figure4.15 (a) to (c). However, the differences between the elliptical crack with inclinations and the penny crack are found from K_2 and K_3. The maximum values for both of K_2 and K_3 are found at $\alpha = 0^{\circ}$ in Figure 4.16 and Figure 4.17. It is observed obviously from Figure 4.16 (a) for center elliptical crack with inclinations.

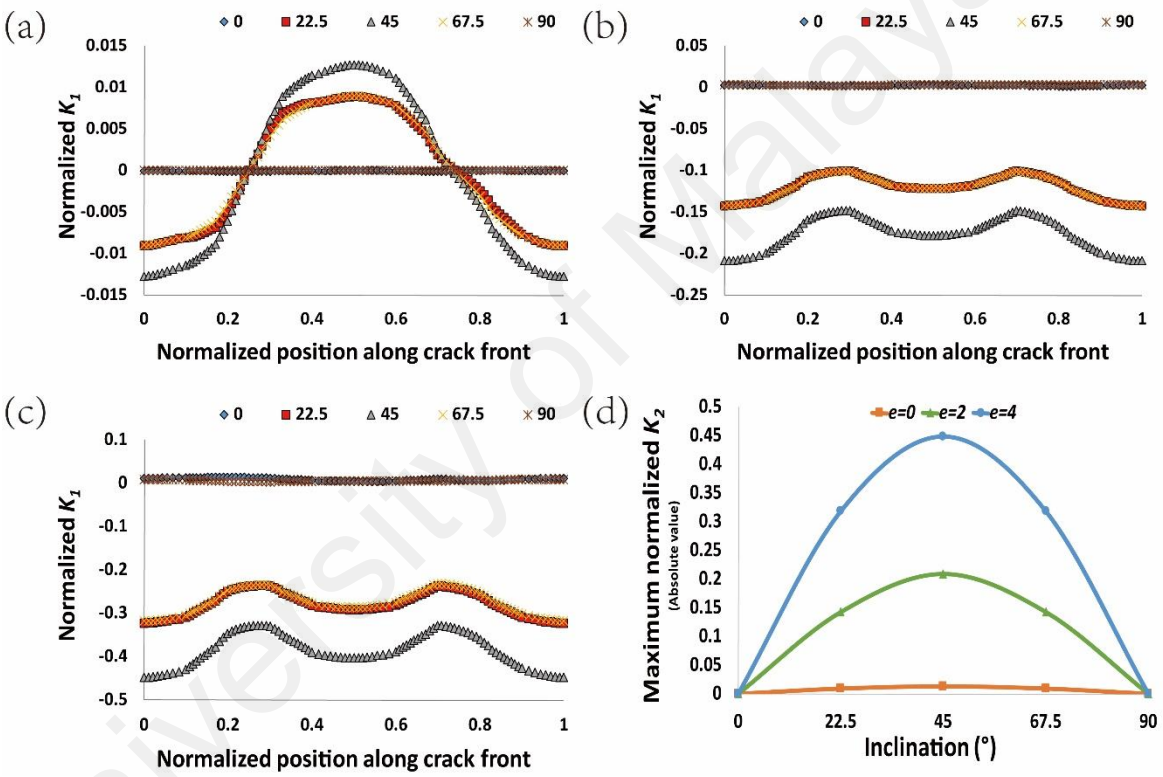

Figure 4.15: (a) K_1 of a center elliptical crack with inclinations; (b) K_1 of inclined elliptical cracks with e = 2 along X'; (c) K_1 of inclined elliptical cracks with e = 4 along X'; (d) $K_1^{\max}$ along X'.

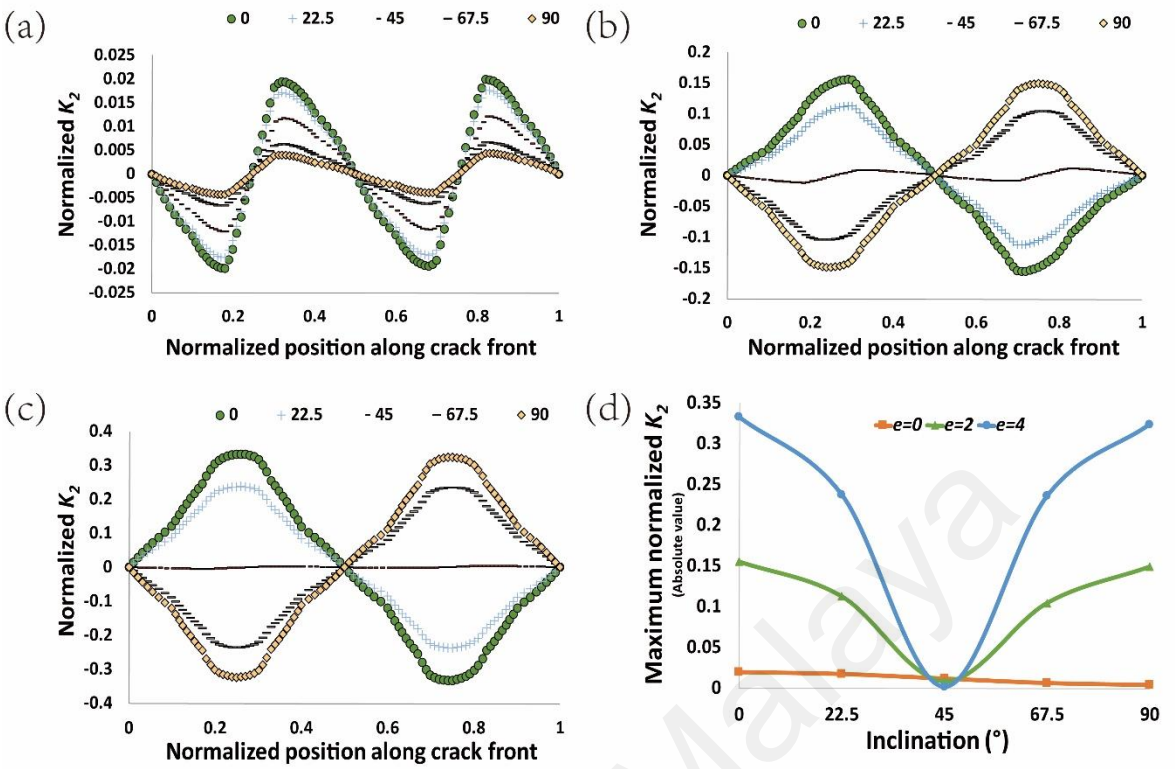

Figure 4.16: (a) K_2 of a center elliptical crack with inclinations; (b) K_2 of inclined elliptical cracks with e = 2 along X'; (c) K_2 of inclined elliptical cracks with e = 4 along X'; (d) $K_2^{\max}$ along X'.

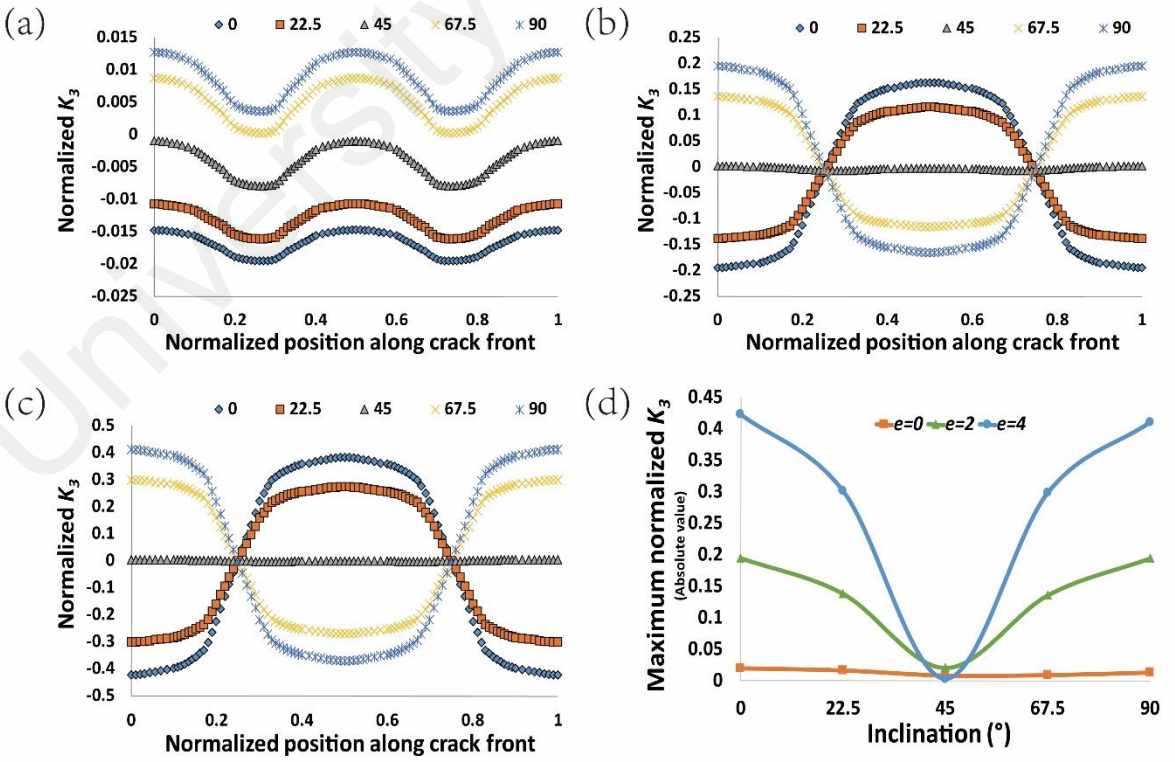

Figure 4.17: (a) K_3 of a center elliptical crack with inclinations; (b) K_3 of inclined elliptical cracks with e = 2 along X'; (c) K_3 of inclined elliptical cracks with e = 4 along X'; (d) $K_3^{\max}$ along X'.

4.7 Effects of different geometry models

As the analysis showed above, the SIFs would be influenced by not only different parameters of cracks but also the geometry among different models. Thus, it is also important to study the effect of the SIFs for embedded crack with eccentricities within different models. Figure 4.18(a) has showed 3 different geometry models which are square bar 1 (10×10 mm^2 for cross section), square bar 2 ($10\sqrt{2} \times 10\sqrt{2}$ mm^2 for cross section) and one cylindrical bar ($10\sqrt{2}$ m for diameter). Eccentric penny cracks with $b = a = 0.5$ mm on the cross section of these three models have been set, in which eccentricities along X and X' (as Figure 4.8 showed) are 2 and 4.071 respectively.

Observation in Figure 4.18 (b) to (e) showed that the value of K_2 and K_3 in a square bar along the X' axis is always greater than the same crack along the X axis even though the eccentricities of them are all same. The reason should be the stress distribution near the edge of the square bar is always higher than near other places (see Figure 4.4 (d)). Also, cracks along the X axis will suffered less deformed and the constraint from two edges of the model, and the less deformation of the crack the less SIFs of it will be obtained.

On the other hand, the different results have been gained from the cylindrical bar, the K_2 and K_3 are smaller than the value of the square bar 1 but higher than the square bar 2 with the same eccentricities since the geometry of it are different with these two square bars. The SIFs is decreasing when the volume of the model is becoming higher since the stress distribution is also decreasing.

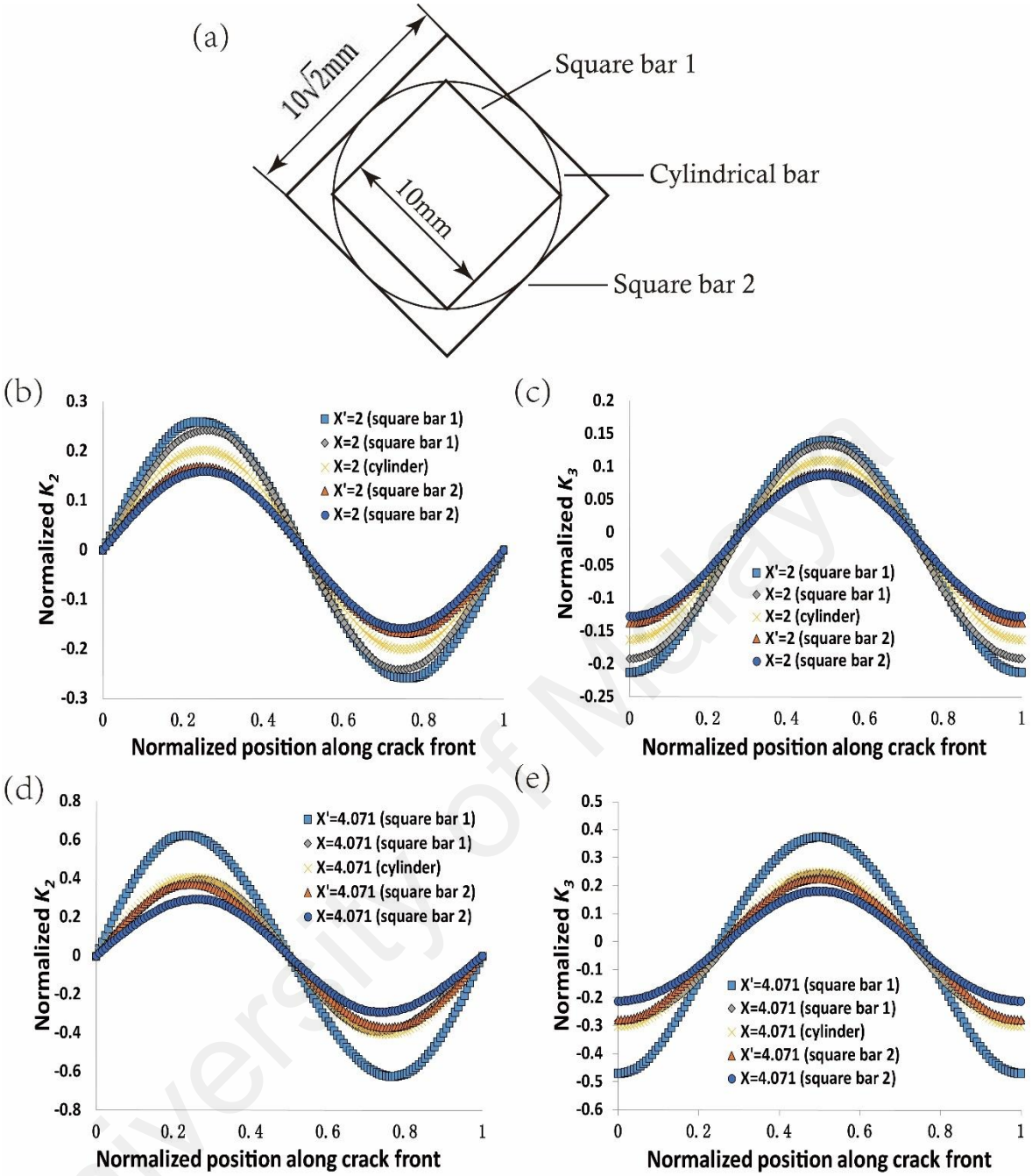

Figure 4.18: (a) Penny crack on cross section of two square bars and a cylindrical bar; (b) K_2 of penny cracks with e = 2 mm; (c) K_3 of penny cracks with e = 2 mm; (d) K_2 of penny cracks with e = 4.071 mm; (e) K_3 of a penny crack with e = 4.071 mm.

CHAPTER 5

CONCLUSIONS & FUTURE WORKS

4.5 Conclusion

Simulation results using BEASY software based on DBEM are presented in Chapter 4. SIFs for elliptical embedded cracks in a square prismatic bar subjected to torsion are evaluated thoroughly by considering elliptical aspect ratio, eccentricity in the sense of an offset from the centroid, and inclination with respect to the normal plane of the centroid axis. Through an effective sampling of locations over 1/8 of the cross-sectional domain, we have presented comprehensive results that could potentially be used to estimate the SIFs for an arbitrary (aspect ratio and inclination) crack located at a general location. Based on the results, some conclusions are made which can be summarized as follows:

1. In general, the results conform to the theory of elasticity.
2. As *b/a* increases, both in-plane and anti-plane, SIF increases and the most severe location is at or close to the apical positions.
3. With offset, K_2 is maximum at a location close to the major axis while K_3 is maximum at a location close to the minor axis.
4. As cracks become inclined, both these maximum values become highest with $\alpha = 90^{\circ}$ for penny cracks, but the $\alpha = 0^{\circ}$ is the maximum value for elliptical cracks with (*b/a* = 2).
5. SIF K_1 due to the inclination is found to be maximum at the apical positions with $\alpha = 45^{\circ}$ as the most severe orientation.
6. The comparisons between different geometry models showed that the SIFs are influenced predominantly by stress distribution especially from the shearing and tearing effects. Nevertheless, the effect of the shape of external boundary is less significant.

4.6 Future works

This work can be extended to the following further studies:

Evaluations of SIFs for different loading such as bending or combination of tension and torsion applied on the square prismatic bar.

Fatigue crack growth analysis of an embedded crack in a square prismatic bar for parameters and types of loadings designed.

REFERENCES

Aliabadi, MH. (1997). Boundary element formulations in fracture mechanics. *Applied Mechanics Reviews, 50*(2), 83-96.

Atroshchenko, E, Potapenko, S, & Glinka, G. (2009). Stress intensity factor for an embedded elliptical crack under arbitrary normal loading. *International Journal of Fatigue, 31*(11), 1907-1910.

Brancati, A, Aliabadi, MH, & Benedetti, I. (2009). Hierarchical adaptive cross approximation GMRES technique for solution of acoustic problems using the boundary element method. *Computer Modeling in Engineering and Sciences (CMES), 43*(2), 149.

Brebbia, CA, & Butterfield, R. (1978). Formal equivalence of direct and indirect boundary element methods. *Applied Mathematical Modelling, 2*(2), 132-134.

Carson, WG. (1980). The other price of Britain's oil: Regulating safety on offshore oil installations in the British sector of the North Sea. *Crime, Law and Social Change, 4*(3), 239-266.

Cherepanov, Genady P. (1967). Crack propagation in continuous media: PMM vol. 31, no. 3, 1967, pp. 476–488. *Journal of Applied Mathematics and Mechanics, 31*(3), 503-512.

Chetan, Jadav, Khushbu, Panchal, & Nauman, Moulvi. (2012). The fatigue analysis of a vehicle suspension system-A review article. *International Journal of Advanced Computer Research, 2*(4).

Choi, Myung-Jin, & Cho, Seonho. (2014). Isogeometric shape design sensitivity analysis of stress intensity factors for curved crack problems. *Computer Methods in Applied Mechanics and Engineering, 279*, 469-496.

Citarella, R, & Cricrì, G. (2010). Comparison of DBEM and FEM crack path predictions in a notched shaft under torsion. *Engineering Fracture Mechanics, 77*(11), 1730-1749.

Costabel, Martin. (1987). *Symmetric methods for the coupling of finite elements and boundary elements (invited contribution)*: Springer.

Cruse, TA. (1969). Numerical solutions in three dimensional elastostatics. *International journal of solids and structures, 5*(12), 1259-1274.

Da Fonte, Manuel, & De Freitas, Manuel. (1999). Stress intensity factors for semi-elliptical surface cracks in round bars under bending and torsion. *International Journal of Fatigue, 21*(5), 457-463.

Domínguez, J, & Ariza, MP. (2000). A direct traction BIE approach for three-dimensional crack problems. *Engineering Analysis with Boundary Elements, 24*(10), 727-738.

Dong, Yuexing, Wang, Zongmin, & Wang, Bo. (1997). On the computation of stress intensity factors for interfacial cracks using quarter-point boundary elements. *Engineering fracture mechanics, 57*(4), 335-342.

Dubrova, Elena. (2013). *Fault-tolerant design*: Springer.

Erdogan, F. (1983). Stress intensity factors. *Journal of Applied Mechanics, 50*(4b), 992-1002.

Erdogan, M Emin. (2000). A note on an unsteady flow of a viscous fluid due to an oscillating plane wall. *International Journal of Non-Linear Mechanics, 35*(1), 1-6.

Fischer-Cripps, Anthony C. (2000). *Introduction to contact mechanics*: Springer.

Freudenthal, Alfred M. (1973). Fatigue and fracture mechanics. *Engineering Fracture Mechanics, 5*(2), 403-414. doi: http://dx.doi.org/10.1016/0013-7944(73)90030-1

Gramling, Robert, & Freudenburg, William R. (2006). Attitudes toward offshore oil development: A summary of current evidence. *Ocean & coastal management, 49*(7), 442-461.

Griffith, Alan A. (1921). The phenomena of rupture and flow in solids. *Philosophical transactions of the royal society of london. Series A, containing papers of a mathematical or physical character, 221*, 163-198.

Hohenester, Ulrich, & Trügler, Andreas. (2012). MNPBEM–A Matlab toolbox for the simulation of plasmonic nanoparticles. *Computer Physics Communications, 183*(2), 370-381.

Hsiao, George C. (2006). Boundary element methods—An overview. *Applied numerical mathematics, 56*(10), 1356-1369.

Hutchinson, JW. (1968). Singular behaviour at the end of a tensile crack in a hardening material. *Journal of the Mechanics and Physics of Solids, 16*(1), 13-31.

Imran, M, Lim, SF Eric, Putra, IS, Ariffin, AK, Tan, CJ, & Purbolaksono, J. (2015). Assessment of a planar inclusion in a solid cylinder. *Engineering Failure Analysis, 48*, 236-246.

Irwin, George R. (1997). Analysis of stresses and strains near the end of a crack traversing a plate. *SPIE MILESTONE SERIES MS, 137*, 167-170.

Jaswon, MA, Maiti, M, & Symm, GT. (1967). Numerical biharmonic analysis and some applications. *International Journal of Solids and Structures, 3*(3), 309-332.

Johnson, Barry W. (1984). Fault-tolerant microprocessor-based systems. *IEEE Micro, 4*(6), 6-21.

Kim, Woo Hyung, & Laird, C. (1978). Crack nucleation and stage I propagation in high strain fatigue—II. Mechanism. *Acta Metallurgica, 26*(5), 789-799.

Korkmaz, Sinan. (2010). *Uniform material law: extension to high-strength steels: a methodology to predict fatigue life of high-strength steels*.

Le Delliou, Patrick, & Barthelet, Bruno. (2007). New stress intensity factor solutions for an elliptical crack in a plate. *Nuclear engineering and design, 237*(12), 1395-1405.

Lee, Doo-Sung. (2007). The effect of an elliptic crack on the stress distribution in a long circular cylinder. *International Journal of Solids and Structures, 44*(11–12), 4110-4119. doi: http://dx.doi.org/10.1016/j.ijsolstr.2006.11.009

Leonel, Edson Denner, Venturini, Wilson Sergio, & Chateauneuf, Alaa. (2011). A BEM model applied to failure analysis of multi-fractured structures. *Engineering Failure Analysis, 18*(6), 1538-1549.

Li, Rongsheng, Gao, Zengliang, & Lei, Yuebao. (2012). A Global Limit Load Solution for Plates With Embedded Off-Set Elliptical Cracks Under Combined Tension and Bending. *Journal of Pressure Vessel Technology, 134*(1), 011204.

Li, Wen-Chin, Harris, Don, & Yu, Chung-San. (2008). Routes to failure: analysis of 41 civil aviation accidents from the Republic of China using the human factors analysis and classification system. *Accident Analysis & Prevention, 40*(2), 426-434.

Lin, XB, & Smith, RA. (1999). Stress intensity factors for corner cracks emanating from fastener holes under tension. *Engineering Fracture Mechanics, 62*(6), 535-553.

Liu, Xiao Yu, Qian, Cai Fu, Li, Hui Fang, & Zheng, Hui. (2011). *Calculation of the Stress Intensity Factors for Elliptical Cracks Embedded in a Weld under Tensile Loading I: Single Crack.* Paper presented at the Advanced Materials Research.

Livieri, Paolo, & Segala, Fausto. (2010). An analysis of three-dimensional planar embedded cracks subjected to uniform tensile stress. *Engineering Fracture Mechanics, 77*(11), 1656-1664.

Matthew, J. (2000). Donachie. *Titanium: A Technical Guide, second ed., ASM International, 10*, 9781118985960.

Mi, Y, & Aliabadi, MH. (1992). Dual boundary element method for three-dimensional fracture mechanics analysis. *Engineering Analysis with Boundary Elements, 10*(2), 161-171.

Miranda, ACO, Meggiolaro, MA, Castro, JTP, Martha, LF, & Bittencourt, TN. (2003). Fatigue life and crack path predictions in generic 2D structural components. *Engineering Fracture Mechanics, 70*(10), 1259-1279.

Montenegro, Hugo López, Cisilino, Adrián, & Otegui, José Luis. (2006). A weight function methodology for the assessment of embedded and surface irregular plane cracks. *Engineering fracture mechanics, 73*(17), 2662-2684.

Nageswaran, Shan. (1990). Beasy—An Analysis Tool for Design Engineers *Boundary Element Methods in Engineering* (pp. 240-259): Springer.

Newman Jr, JC, & Raju, IS. (1986). Stress-intensity factor equations for cracks in three-dimensional finite bodies subjected to tension and bending loads. *Computational methods in the mechanics of fracture, 2*, 311-334.

Orowan, Et. (1949). Fracture and strength of solids. *Reports on progress in physics, 12*(1), 185.

Paris, Paul C, Gomez, Mario P, & Anderson, William E. (1961). A rational analytic theory of fatigue. *The trend in engineering, 13*(1), 9-14.

Pasquetti, Richard, & Peres, Noele. (2015). A penalty model of synthetic micro-jet actuator with application to the control of wake flows. *Computers & Fluids, 114*, 203-217. doi: http://dx.doi.org/10.1016/j.compfluid.2015.02.019

Qian, Xudong. (2010). K I–T estimations for embedded flaws in pipes–Part I: Axially oriented cracks. *International Journal of Pressure Vessels and Piping, 87*(4), 134-149.

Rice, James R. (1968). A path independent integral and the approximate analysis of strain concentration by notches and cracks. *Journal of applied mechanics, 35*(2), 379-386.

Rizzo, Frank J. (1967). An integral equation approach to boundary value problems of classical elastostatics. *Quart. Appl. Math, 25*(1), 83-95.

Rotem, A. (1991). The fatigue behavior of composite laminates under various mean stresses. *Composite structures, 17*(2), 113-126.

Rutherford, David B. (1992). What Do You Mean-It's Fail-safe? *Vancouver*.

Shallcross, David C. (2013). Using concept maps to assess learning of safety case studies: the Eschede train disaster. *INTERNATIONAL JOURNAL OF ENGINEERING EDUCATION, 29*(5), 1281-1293.

Shigley, Joseph Edward, Mischke, Charles R, Budynas, Richard G, Liu, Xiangfeng, & Gao, Zhi. (1989). *Mechanical engineering design* (Vol. 89): McGraw-Hill New York.

Takahashi, Akiyuki, & Ghoniem, Nasr M. (2013). Fracture mechanics of propagating 3-D fatigue cracks with parametric dislocations. *Philosophical Magazine, 93*(20), 2662-2679.

Timoshenko, SP, & Goodier, JN. (1970). Theory of Elasticity (3rd) McGraw-Hill. *New York*.

Torshizian, Mohammad R, & Kargarnovin, Mohammad H. (2014). The mixed-mode fracture mechanics analysis of an embedded arbitrary oriented crack in a two-dimensional functionally graded material plate. *Archive of Applied Mechanics, 84*(5), 625-637.

Trevelyan, J. (1992). The Effective Use and Accuracy of BEASY'S Discontinuous Boundary Elements for Fracture Mechanics Analysis *Boundary Element Technology VII* (pp. 635-649): Springer.

Vijayakumar, K, Wylie, SR, Cullen, JD, Wright, CC, & Ai-Shamma'a, AI. (2009). *Non invasive rail track detection system using Microwave sensor.* Paper presented at the Journal of Physics: Conference Series.

Wöhler, A. (1870). Über die Festigkeitsversuche mit Eisen und Stahl. Auf Anordnung des Ministers für Handel, Gewerbe u. öffentl. Arbeiten, Grafen Itzenblitz, angestellt. *Ernst und Korn, Berlin*.

Wanderlingh, Arturo I. (1986). Technical Note: Comparison of boundary element and finite element methods for linear stress analysis—technical program results. *Engineering analysis, 3*(3), 177-180.

Wang, Xin, & Glinka, Grzegorz. (2009). Determination of approximate point load weight functions for embedded elliptical cracks. *International Journal of Fatigue, 31*(11), 1816-1827.

Wearing, JL, & Ahmadi-Brooghani, SY. (1999). The evaluation of stress intensity factors in plate bending problems using the dual boundary element method. *Engineering analysis with boundary elements, 23*(1), 3-19.

Yan, Xiangqiao. (2006). Numerical analysis of a few complex crack problems with a boundary element method. *Engineering Failure Analysis, 13*(5), 805-825.

Yan, Xiangqiao. (2010). A boundary element analysis for stress intensity factors of multiple circular arc cracks in a plane elasticity plate. *Applied Mathematical Modelling, 34*(10), 2722-2737.

Yan, Xiangqiao, & Liu, Baoliang. (2012). Fatigue growth modeling of cracks emanating from a circular hole in infinite plate. *Meccanica, 47*(1), 221-233.

Yavari, Vahid, Rajabi, Iraj, Daneshvar, Farshad, & Kadivar, Mohammad Hassan. (2009). On the stress distribution around the hole in mechanically fastened joints. *Mechanics Research Communications, 36*(3), 373-380.

Yazdi, A Kamali, & Shooshtari, A. (2014). Analysis of cracked truss type structures. *ASIAN JOURNAL OF CIVIL ENGINEERING (BHRC), 15*(4), 517-533.